

## Stable terminal methylene complexes of osmium(II) and ruthenium(II). The unexpected preferential migration of a $\sigma$ -aryl ligand to carbon monoxide rather than to methylene

D. Scott Bohle, George R. Clark, Clifton E.F. Rickard, Warren R. Roper\* and L. James Wright

*Department of Chemistry, The University of Auckland, Private Bag, Auckland (New Zealand)*

(Received April 8th, 1988)

### Abstract

Isolable methylene complexes  $MCl(\eta^2-C[O]R)(=CH_2)(PPh_3)_2$  ( $M = Ru$ ;  $R = Ph$ , *o*-tolyl, *p*-tolyl, **2a–2c**;  $M = Os$ ;  $R = o$ -tolyl, **2d**) result when  $MClR(CO)(PPh_3)_2$ , **1a–1d**, are treated with diazomethane. Halide metathesis of **2a** with lithium bromide or iodide results in the halide substituted methylene complexes  $RuX(\eta^2-C[O]Ph)(=CH_2)(PPh_3)_2$ ,  $X = Br$ , **3a**, and  $X = I$ , **4a**. Carboxylates also substitute for the chloride in **2** but the final products,  $M(CH_2OC[O]R')(R)(CO)(PPh_3)_2$ , **5a–5f** ( $M = Ru, Os$ ;  $R = Ph, p$ -tolyl, *o*-tolyl;  $R' = Me, p$ -tolyl), result from reverse migration of the aryl from the  $\eta^2$ -acyl to the metal and addition of carboxylate to the terminal methylene ligand. A structural study of one of these species,  $Ru(CH_2OC[O]CH_3)(Ph)(CO)(PPh_3)_2$ , **5a**, which crystallizes in monoclinic space group  $P2_1/n$ ,  $a$  14.701(2),  $b$  19.193(3),  $c$  14.881(2) Å,  $\beta$  111.32(1)°,  $Z = 4$ ,  $V$  3911.33 Å<sup>3</sup>, indicates that the aryl ligand is *trans* to the methylene unit.

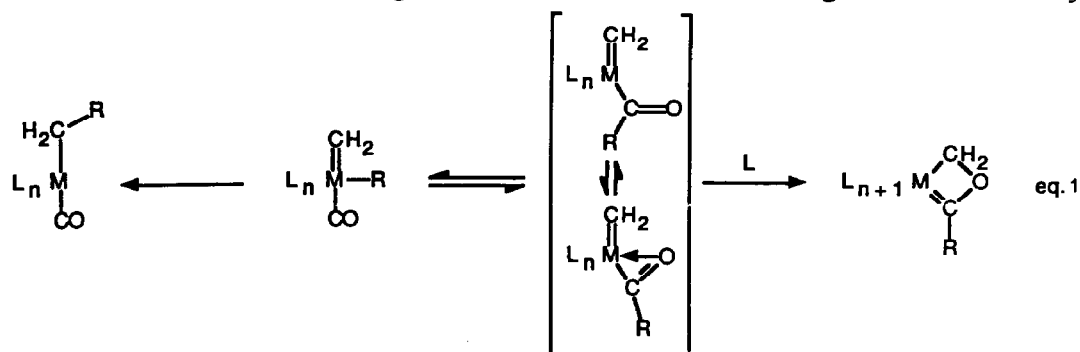
Carbon monoxide and *p*-tolylisocyanide react with **2a–2e** to form  $[M(=C(R)OCH_2)L_2(PPh_3)_2]^+$ , which were isolated as the perchlorate salts **7a**, **7b**, **7d**, **8a** ( $M = Ru, Os$ ;  $R = Ph, o$ -tolyl;  $L = CO, CN$ -*p*-tolyl). These compounds contain the unusual metallaoxetene,  $[M=C(R)OCH_2]$ , ring which results from the ligand sphere combination reactions of the terminal methylene and  $\eta^2$ -acyl ligands. Full details of the crystallographic studies of  $OsCl(\eta^2-C[O]-o$ -tolyl)(=CH<sub>2</sub>)(PPh<sub>3</sub>)<sub>2</sub> and  $[Ru(=C(Ph)OCH_2)(CN-p$ -tolyl)<sub>2</sub>(PPh<sub>3</sub>)<sub>2</sub>]ClO<sub>4</sub> are also reported.

### Introduction

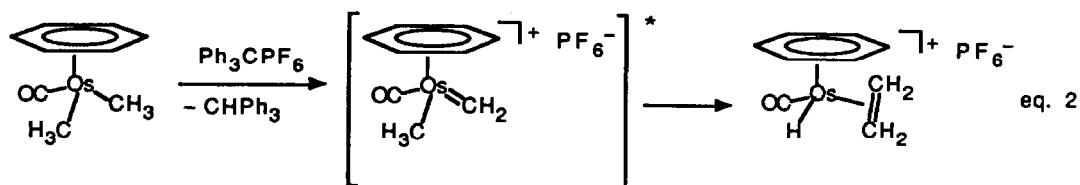
Stable terminal methylene complexes are now known for early and late transition metals with a range of oxidation states and spectator ligands. Nevertheless, these species remain relatively rare and only four structurally characterized examples have been reported [1–4]. The reactivity patterns associated with terminal methylene

complexes include attack by both electrophiles, [2,5] and nucleophiles [6–8], cyclopropanation [9], and migratory insertion, with the observed reactivity being markedly dependent upon the electronic configuration of the metal, the charge of the complex and the spectator ligands. Significantly, examples of the migratory insertion reactions of methylene ligands are limited to  $\eta^2$ -alkene [10],  $\eta^2$ -alkyne [11], methyl [12–14] and hydride [15]. In each of these reactions the involvement of an intermediate cationic terminal methylene complex is only deduced from the products and none of these intermediates has been isolated or detected in solution. For the particular case of the methyl migration, the immediate product, which contains an ethyl ligand, has only been observed in one instance [14] and in the remaining two cases this mechanism is inferred from the presence of a hydride and an  $\eta^2$ -ethylene ligand in the product.

These migratory insertion/ligand sphere combination reactions of the terminal methylene ligand are not only intrinsically interesting but they are also significant because they may model the crucial steps in the methylene polymerization reaction in the Fischer-Tropsch process [16,17]. However, it is often assumed that migratory insertion of an alkyl (or aryl) ligand to a terminal methylene is irreversible and favoured over the related migration to a carbon monoxide ligand. Schematically



shown in eq. 1 is the situation where R can migrate to either of these ligands and the general expectation is that these linked equilibria and migrations will be driven towards the left. Indeed, in one of the methyl examples above the products (eq. 2) arise from the preferential migration to the methylene ligand [13]. Also shown in eq.

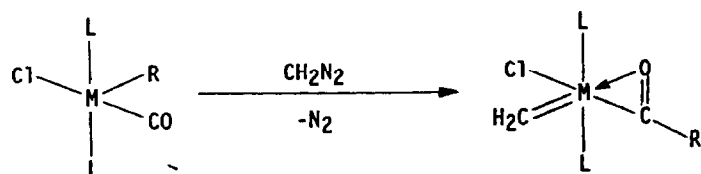


\* proposed intermediate

1 is one of a host of related side-reactions, that is, a methylene/ $\eta^2$ -acyl ligand combination, that potentially may accompany the initial migratory insertion of R to carbon monoxide.

Against these expectations the introduction of a terminal methylene ligand into the  $\sigma$ -aryl complex  $MClR(CO)(PPh_3)_2$  results in aryl migration to the carbon monoxide ligand to give an  $\eta^2$ -acyl complex only and not the benzyl complex which

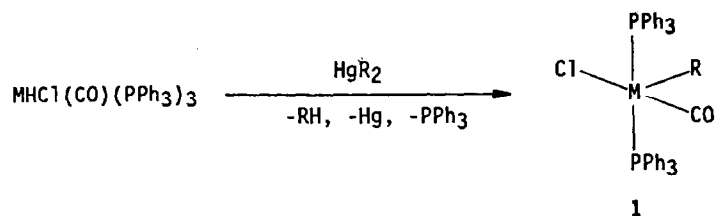
would be expected to arise from the migration of R to the methylene ligand. This reaction is accomplished by treating these coordinatively unsaturated  $\sigma$ -aryl species with diazomethane to afford  $MCl(\eta^2-C[O]R)(=CH_2)(PPh_3)_2$ :



Herein we describe: (1) Instances where there is preferential migration of an aryl group to carbon monoxide and not to the methylene ligand. (2) Full details of the synthesis and reactions of these methylene complexes and the crystal structure of one of these,  $OsCl(\eta^2-C[O]-o\text{-tolyl})(=CH_2)(PPh_3)_2$ ; (3) The crystal structure of  $Ru(CH_2OC[O]CH_3)(Ph)(CO)(PPh_3)_2$ , which results from acetate addition to the  $Ru=CH_2$  bond and substitution of chloride; (4) Full details of the preparation and the crystal structure of the metallaoxetene containing complex  $[Ru(=C(Ph)OCH_2)-(CN-p\text{-tolyl})_2(PPh_3)_2]ClO_4$  which results from combination of the methylene and acyl ligands. Some aspects of this work have been published in preliminary form previously [18].

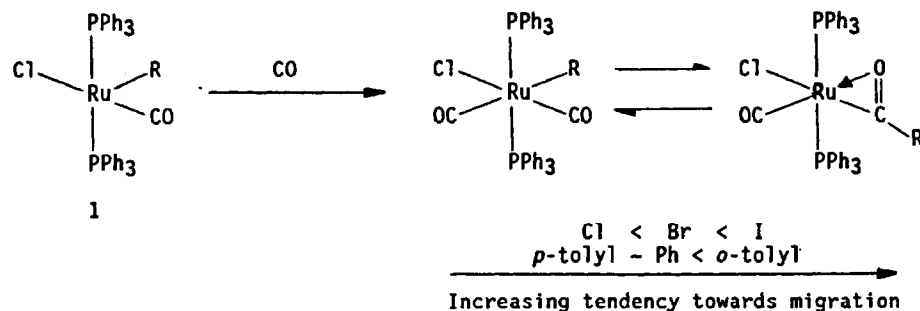
## Results and discussion

In prior work [19–21] we have reported the preparation and migratory insertion reactions of a series of coordinatively unsaturated divalent ruthenium and osmium aryl complexes  $MXR(CO)(PPh_3)_2$  (**1**). These complexes are prepared in high yield by treating  $MHCl(CO)(PPh_3)_3$  with  $HgR_2$ :

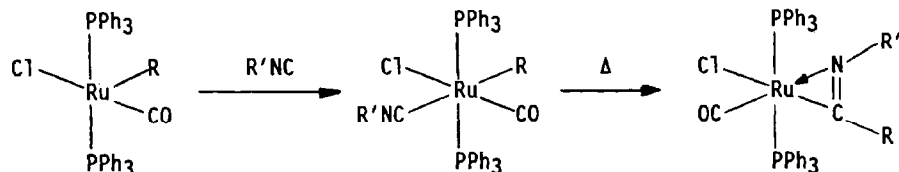


M = Ru, Os; R = Ph, *p*-tolyl, *o*-tolyl

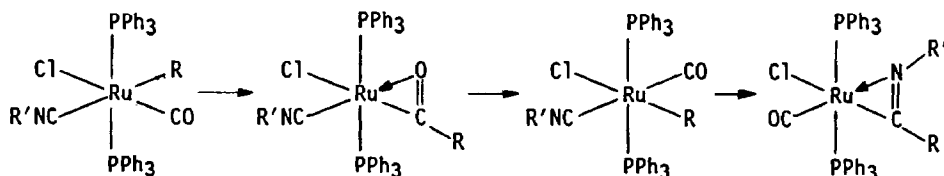
Carbonylation of the ruthenium complexes results in a rapidly established equilibrium mixture of an aryl/dicarbonyl species and an  $\eta^2$ -acyl/carbonyl species. The position of this equilibrium is markedly dependent upon X and R:



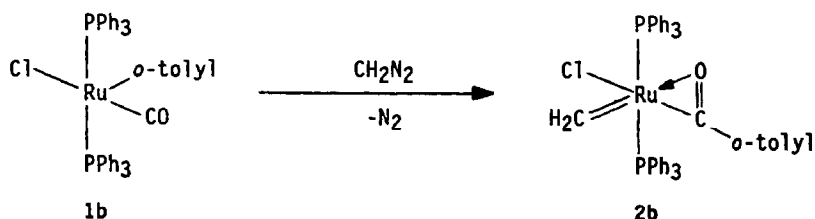
On the other hand the osmium analogues of **1** carbonylate to give the dicarbonyl/aryl isomer as the only detectable species. Addition of isocyanide to the ruthenium species initially results in an isocyanide complex. On heating this then rearranges to an  $\eta^2$ -iminoacyl complex:



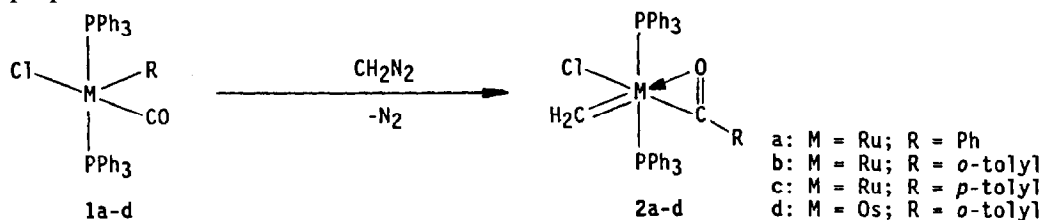
The step-wise formation of these  $\eta^2$ -iminoacyl complexes is significant as it illustrates the high mobility of ligands within the coordination sphere of  $\text{MClR}(\text{CO})(\text{L})(\text{PPh}_3)_2$  ( $\text{L} = \pi$ -acceptor ligand). The isocyanide must originally coordinate *trans* to R and the formation of a  $\eta^2$ -iminoacyl ligand requires a *cis* configuration of the aryl and isocyanide ligands. This arrangement may arise from the reversible migration of the aryl group on and off the carbon monoxide:



The work reported herein was prompted by the discovery that the coordinatively unsaturated ruthenium(II) complex  $\text{RuCl}(o\text{-tolyl})(\text{CO})(\text{PPh}_3)_2$  (**1b**) reacts rapidly with diazomethane. There is a steady evolution of nitrogen and within minutes the solution has a deep black colour. After column chromatography on silica gel the stable terminal methylene complex **2b** can be isolated as yellow-orange plate-like crystals:



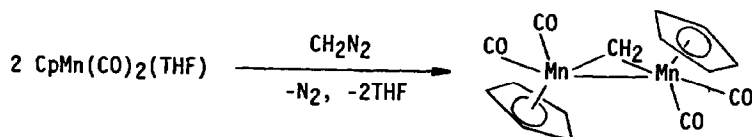
After this initial discovery a range of coordinatively unsaturated  $\sigma$ -aryl complexes for both osmium and ruthenium was treated under similar conditions to test the generality of the above reaction. As a result of these experiments with  $\text{R} = \text{Ph}$ , *p*-tolyl, *o*-tolyl for both metals, the four terminal methylene complexes, **2a–2d**, were prepared:



With appropriate conditions, the yield of **2a–d** can be boosted to between 72–56%. This entails slow, drop-wise addition of freshly prepared ether solutions of diazomethane to solutions of **1a–1d** at room temperature. Conducting the reaction at lower temperatures or rapid addition of diazomethane results in decreased yields. In each reaction there are significant quantities of black decomposition products which must be removed by chromatography. The identity of these materials is unknown.

The formation of **2a–2d** involves several steps, among which are the following: (1) Coordination of diazomethane to the metal. (2) Migration of the aryl group to the carbon monoxide. (3) Elimination of dinitrogen.

It is unlikely that free methylene is involved in this reaction as there are no unambiguous examples of transition metals that “trap” a free carbene by coordination. Furthermore, there are many precedents for the formation of diazoalkane complexes and examples that are  $\eta^1$ -*N* bound,  $\eta^2$ -*N,N* bound and  $\eta^2$ -*C,N* bound are known. Often treating transition metal substrates with diazomethane leads to  $\mu_2$ -methylene bridging complexes rather than terminal complexes [22]:



The limitation of the reactivity of **1** with diazomethane to the four cases **1a–1d** suggests that the key step in the formation of **2a–2d** is the migratory insertion involving the carbonyl and the aryl ligands. For example, although three ruthenium(II) terminal methylene complexes **2a–2c** can be prepared only a single osmium example **2d**, with R = *o*-tolyl, is formed under the same conditions. It is generally recognized that the reactivity towards carbonyl insertion decreases on descending a transition metal triad [23]. The osmium complex **2d** is unique in that it is the only  $\eta^2$ -acyl complex that has been reported for this metal. The large steric pressure exerted by the *o*-tolyl group may be responsible for aryl migration being favourable in this instance.

To test the importance of the migratory insertion reaction in the preparation of **2a–2d**, very closely related five coordinate aryl thiocarbonyl complexes of osmium and ruthenium were treated with diazomethane under the same conditions as for **1a–1d**. It is well known that the migratory insertion reaction for thiocarbonyls is more facile than for carbonyls [24] and it was expected that methylene complexes with  $\eta^2$ -thioacyl ligands should form more readily, and perhaps in higher yields, than do the acyl complexes. Unfortunately, this was not the case, and even under a variety of conditions treating either RuCl(*p*-tolyl)(CS)(PPh<sub>3</sub>)<sub>2</sub>, or OsCl(*o*-tolyl)(CS)(PPh<sub>3</sub>)<sub>2</sub> with diazomethane lead to vigorous nitrogen evolution and ill-defined products which could not be characterized. Other substrates, all potentially coordinatively unsaturated, which failed to give tractable products on reaction with diazomethane were RuCl(CF<sub>3</sub>)(NCCH<sub>3</sub>)(CO)(PPh<sub>3</sub>)<sub>2</sub>, RuCl(*trans*- $\beta$ -styryl)(CO)(PPh<sub>3</sub>)<sub>2</sub>, [Os(NO)(CO)(PPh<sub>3</sub>)<sub>3</sub>][ClO<sub>4</sub>] and MHCl(CO)(PPh<sub>3</sub>)<sub>3</sub> (M = Ru, Os).

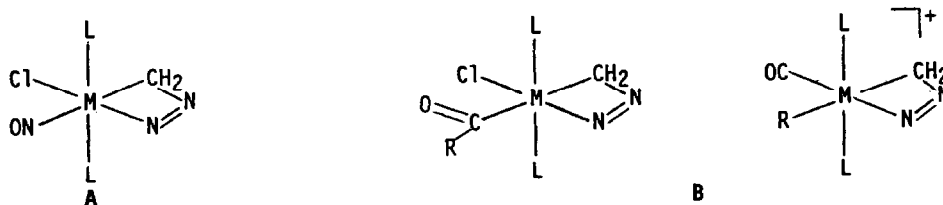
The only other substrates which we have found which react with diazomethane to give stable terminal methylene complexes are RuCl(NO)(PPh<sub>3</sub>)<sub>2</sub> and OsCl(NO)(PPh<sub>3</sub>)<sub>3</sub> [2]. Two factors may account for the fact that only the two

generalized compound types  $MCl(NO)(PPh_3)_2$  and  $MCl(R)(CO)(PPh_3)_2$  have been found which react with diazomethane in this manner:

(1) Both compounds are coordinatively unsaturated.

(2) Both compounds have potentially non-innocent ligands which may allow for access to what are formally 14 electron species with two vacant coordination sites.

In the synthesis of  $MCl(NO)(=CH_2)(PPh_3)_2$  the intermediate **A**, with a  $\eta^2$ -C,N bound diazomethane ligand has been postulated [25]:



A stable  $(CF_3)_2C=N=N$  adduct of  $IrCl(N_2)(PPh_3)_2$  is thought [26] to have a geometry similar to that depicted in **A**. Formation of **A** requires non-innocence on the part of the nitrosyl ligand to allow for the coordination of both ends of diazomethane. Similar intermediates, **B**, can arise in the reaction of  $MClR(CO)(PPh_3)_2$  with diazomethane either by migration of the aryl, to give a  $\eta^1$ -acyl intermediate, or by loss of chloride, to give a cationic aryl-carbonyl intermediate. The flexible coordination environment in both of these substrates may be a general requirement for the successful use of diazomethane to prepare terminal methylene complexes. The formation of  $IrI(=CH_2)(CO)(PPh_3)_2$  from  $IrI(CO)(PPh_3)_2$  and diazomethane [2], can be accounted for in terms of a 14 electron intermediate which might form by dissociation of the iodide ligand.

### Structural characterization of $OsCl(\eta^2-C[O]-o\text{-tolyl})(=CH_2)(PPh_3)_2$

Although all of the methylene complexes **2a–2d** are air-stable crystalline solids, solutions of **2a–2d**, even in rigorously dried and deoxygenated solvents, begin to blacken within 2 h at room temperature. However, crystals suitable for X-ray diffraction were obtained (as outlined in the experimental section) and crystallographic data for all three of the diffraction studies described in this paper are collected in Table 1. The full molecular structure of **2d** is shown in Fig. 1, and bond length, bond angle and atomic position data are presented in Tables 2, 3 and 4, respectively. As expected, **2d** has mutually *trans* triphenylphosphine ligands, and the two carbon donors are oriented *cis* to one another. This latter feature is expected to reduce the competition for  $\pi$ -bonding electron density. Figure 2, which is a view of the plane containing the osmium as well as the methylene,  $\eta^2$ -acyl and chloride ligands, illustrates the distortion of the in-plane geometry away from square planar, towards an almost trigonal planar arrangement for the chlorine and the two carbon atoms. Two other structurally characterized ruthenium  $\eta^2$ -acyl complexes,  $RuI(\eta^2-C[O]R)(CO)(PPh_3)_2$ , ( $R = Me, p\text{-tolyl}$ ) also show similar distortions. Table 5 contrasts these geometries for the three  $\eta^2$ -acyl complexes, and it can be seen that in each case the angle between the chloride and the CO or  $CH_2$  ligand,  $\alpha$  in Table 5, is considerably greater than  $90^\circ$ . Thus, the overall configuration of **2d** closely resembles the geometry of related  $\eta^2$ -acyl complexes.

Table 1

Data for the X-ray diffraction studies

	2d	5a	8a
<i>Crystal data</i> <sup>a</sup>			
crystal system	orthorhombic	monoclinic	monoclinic
space group	<i>Pca</i> 2 <sub>1</sub>	<i>P</i> 2 <sub>1</sub> / <i>n</i>	<i>P</i> 2 <sub>1</sub> / <i>n</i>
<i>a</i> (Å)	24.346(3)	14.701(2)	14.871(3)
<i>b</i> (Å)	9.632(1)	19.193(3)	19.534(3)
<i>c</i> (Å)	15.716(4)	14.881(2)	18.601(4)
$\beta$ (°)	–	111.32(1)	97.07(2)
<i>V</i> (Å <sup>3</sup> )	3685.4	3911.33	5362.31
<i>Z</i>	4	4	4
molecular weight	882.65	803.84	1163.52
$\rho$ (calcd) (g cm <sup>-3</sup> )	1.59	1.37	1.40
collection temperature (°C)	–150	25	–140
<i>Measurement of intensity data</i>			
radiation	Monochromated Mo- <i>K</i> $\alpha$ ( $\lambda$ 0.71069 Å)		
scan type	$\omega$ (crystal)– $2\theta$ (counter)		
$2\theta$ range (°)	3–54	3–50	3–50
reflections collected	3648[2615 > 2 $\sigma$ ( <i>I</i> )]	5332[3021 > 3 $\sigma$ ( <i>I</i> )]	9441[6545 > 3 $\sigma$ ( <i>I</i> )]
absorption coefficient (cm <sup>-1</sup> )	38.6	5.2	5.3

<sup>a</sup> Unit cell parameters were obtained from a least squares fit to the setting angles of 25 reflections.

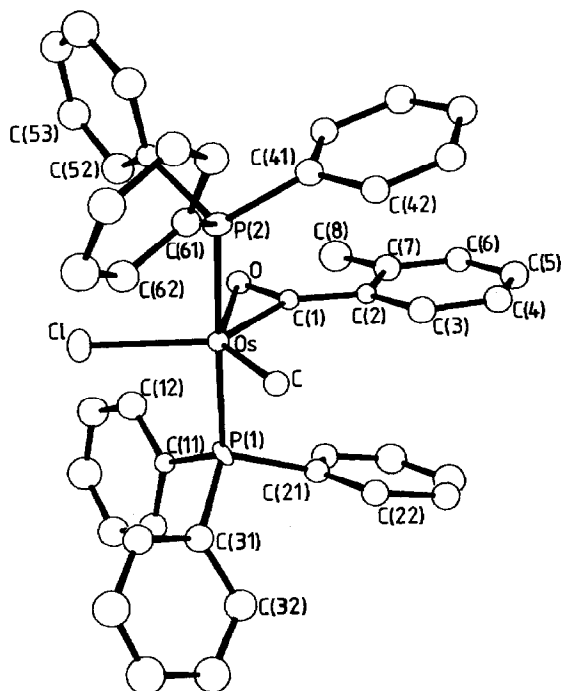


Fig. 1. Molecular structure of OsCl( $\eta^2$ -C[O]-*o*-tolyl)(=CH<sub>2</sub>)(PPh<sub>3</sub>)<sub>2</sub> (2d).

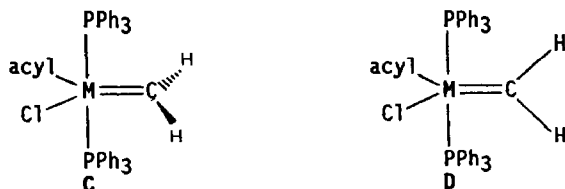
Table 2

Bond lengths for OsCl( $\eta^2$ -C[O]-*o*-tolyl)(=CH<sub>2</sub>)(PPh<sub>3</sub>)<sub>2</sub> (**2d**)

Bond lengths involving osmium ( $\text{\AA}$ )						
P(1)–Os	2.350(2)	C–Os	1.856(12)			
P(2)–Os	2.356(2)	O–Os	2.423(9)			
C(1)–Os	2.009(11)	Cl–Os	2.401(3)			
Bond lengths involving the $\eta^2$ -acyl ligand ( $\text{\AA}$ )						
O–C(1)	1.22(1)	C(2)–C(1)	1.44(2)			
C(3)–C(2)	1.41(2)	C(7)–C(2)	1.42(2)			
C(3)–C(4)	1.40(2)	C(4)–C(5)	1.38(2)			
C(5)–C(6)	1.41(2)	C(6)–C(7)	1.37(2)			
C(7)–C(8)	1.48(2)					
Bond lengths involving triphenylphosphine ligands ( $\text{\AA}$ )						
C(11)–P(1)	1.78(2)	C(41)–P(2)	1.79(2)			
C(21)–P(1)	1.87(2)	C(51)–P(2)	1.87(2)			
C(31)–P(1)	1.84(1)	C(61)–P(2)	1.85(1)			
<i>i</i>						
	1	2	3	4	5	6
C(i1)–C(i2)	1.39(2)	1.36(2)	1.46(2)	1.43(2)	1.37(2)	1.40(2)
C(i1)–C(i6)	1.41(2)	1.37(2)	1.38(2)	1.42(2)	1.45(2)	1.36(2)
C(i2)–C(i3)	1.43(2)	1.42(2)	1.45(2)	1.36(2)	1.41(2)	1.42(2)
C(i3)–C(i4)	1.38(2)	1.39(2)	1.41(3)	1.42(2)	1.38(2)	1.39(2)
C(i4)–C(i5)	1.44(2)	1.36(2)	1.36(2)	1.38(2)	1.37(2)	1.37(2)
C(i5)–C(i6)	1.38(2)	1.39(2)	1.40(2)	1.43(2)	1.42(2)	1.44(2)

The metal–carbon bond length for the methylene ligand is at the short end of the range found for structurally characterized osmium carbene complexes. Table 6 contrasts this structural feature with data for complexes with osmium–carbon multiple bonds, and with other methylene ligands. Interpretation of these data is complicated by the high esd's that are often found for direct metal–carbon bonds. In this case the difference in the Os–CH<sub>2</sub> bond lengths for OsCl(NO)(=CH<sub>2</sub>)(PPh<sub>3</sub>)<sub>2</sub> and **2d** is just barely significant.

The two hydrogen atoms of the methylene ligand were not located by Fourier difference methods and consequently it is not possible to firmly establish the equilibrium orientation of the methylene plane. Two extreme orientations, either orthogonal to **C**, or coplanar with **D**, the triphenylphosphine axis, are expected



on orbital symmetry grounds [32]. It has not been possible to unambiguously distinguish between these two configurations by using <sup>1</sup>H NMR spectroscopy. The observed resonance for the methylene protons, a sharp low-field triplet at 25 °C (e.g.  $\delta$ , 15.73 ppm, <sup>3</sup>J(HP) 13.8 Hz for **2a**) does not exhibit any temperature dependent behaviour when cooled to –55 °C. This observation does not exclude configuration **C** if rotation around the M=CH<sub>2</sub> bond is rapid on the NMR time scale. However,



Table 3

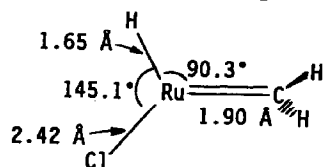
Bond angles for OsCl( $\eta^2$ -C[O]-*o*-tolyl)(=CH<sub>2</sub>)(PPh<sub>3</sub>)<sub>2</sub> (**2d**)

<i>Angles at osmium (°)</i>			
C–Os–P(1)	89.6(4)	P(2)–Os–P(1)	177.2(3)
C–Os–P(2)	87.6(4)	C(1)–Os–P(1)	90.7(4)
C–Os–Cl(1)	109.8(5)	C(1)–Os–P(2)	90.0(4)
C–Os–Cl	120.3(4)	C(1)–Os–Cl	129.9(4)
C–Os–O	140.0(4)	C(1)–Os–O	30.2(4)
Cl–Os–P(1)	90.2(3)	O–Os–P(1)	90.0(2)
Cl–Os–P(2)	91.4(3)	O–Os–P(2)	91.9(2)
Cl–Os–O	99.7(2)		
<i>Angles involving the <math>\eta^2</math>-acyl ligand (°)</i>			
C(1)–O–Os	55.8(6)	C(2)–C(3)–C(4)	119.8(1.1)
O–C(1)–Os	94.0(7)	C(3)–C(4)–C(5)	120.1(1.3)
C(2)–C(1)–Os	140.2(9)	C(4)–C(5)–C(6)	120.1(1.2)
O–C(1)–C(2)	125.6(1.0)	C(5)–C(6)–C(7)	121.3(1.2)
C(1)–C(2)–C(3)	118.8(1.0)	C(6)–C(7)–C(2)	118.8(1.2)
C(1)–C(2)–C(7)	121.1(1.1)	C(6)–C(7)–C(8)	119.1(1.2)
C(3)–C(2)–C(7)	119.3(1.1)	C(2)–C(7)–C(8)	122.0(1.2)
<i>Angles within the triphenylphosphine ligands (°)</i>			
C(11)–P(1)–Os	118.1(6)	C(41)–P(2)–Os	115.1(7)
C(21)–P(1)–Os	111.6(6)	C(51)–P(2)–Os	113.6(7)
C(31)–P(1)–Os	116.2(3)	C(61)–P(2)–Os	116.7(3)
C(21)–P(1)–C(11)	104.4(5)	C(51)–P(2)–C(41)	101.7(6)
C(31)–P(1)–C(11)	100.8(9)	C(61)–P(2)–C(41)	105.5(1.0)
C(31)–P(1)–C(21)	104.1(1.0)	C(61)–P(2)–C(51)	102.4(9)

the magnitude of the phosphorus-hydrogen coupling favours structure **D** since  $^3J(\text{HP})$  varies substantially with the orientation of the alkylidene ligand. Data for related trigonal bipyramidal and octahedral complexes with alkylidene ligands indicate that for the orientation in **D** that  $^3J(\text{HP})$  is in the range 17.0–19.4 Hz [25,28]. For complexes with orientation **C** the values for  $^3J(\text{HP})$  are typically about 2.5 Hz [28,31]. Since the terminal methylene complexes **2a–2d** also have large  $^3J(\text{HP})$  values, it is likely that the orientation of the methylene ligand in these compounds is that shown in **D**.

The question of orientation has a bearing on any discussion of the electronic structure. It is also significant because all structurally characterized related octahedral Os<sup>II</sup> and Ru<sup>II</sup> carbene complexes have the carbene oriented orthogonal, or nearly so, to the metal–tertiary phosphine axis. On the other hand, the structurally characterized Os<sup>0</sup> and Ru<sup>0</sup> carbene complexes have this ligand oriented coplanar with the metal–tertiary phosphine axis. Both of these trends can be rationalized with orbital symmetry arguments [32] and the same arguments can account for the geometry of the related vinylidene and  $\pi$ -adduct structures.

The GVB CI \* optimised structure for RuHCl(=CH<sub>2</sub>) is shown below [33,34]. In



\* GVB CI = generalized valence bond correlation interaction.

Table 4

Atomic positional parameters for  $\text{OsCl}(\eta^2\text{-C}[\text{O}]\text{-}o\text{-tolyl})(=\text{CH}_2)(\text{PPh}_3)_2$  (**2d**)

Atom	x	y	z	Atom	x	y	z
Os	0.50429(1)	0.07611(4)	0.2500	C(31)	0.6359(4)	-0.0857(13)	0.2582(18)
P(1)	0.6008(1)	0.0828(4)	0.2516(7)	C(32)	0.6863(5)	-0.0984(17)	0.3076(11)
P(2)	0.4077(1)	0.0625(3)	0.2544(6)	C(33)	0.7154(6)	-0.2286(18)	0.3005(11)
Cl	0.5059(1)	-0.0070(4)	0.1060(2)	C(34)	0.6942(5)	-0.3344(15)	0.2483(22)
C	0.5056(5)	-0.0483(11)	0.3401(8)	C(35)	0.6442(6)	-0.3248(19)	0.2103(11)
O	0.5017(4)	0.3239(9)	0.2238(5)	C(36)	0.6160(6)	-0.1979(16)	0.2127(10)
C(1)	0.5008(5)	0.2714(12)	0.2946(7)	C(41)	0.3760(8)	0.1565(21)	0.3392(13)
C(2)	0.5020(5)	0.3458(11)	0.3740(7)	C(42)	0.3733(5)	0.0931(15)	0.4215(9)
C(3)	0.4959(5)	0.2711(14)	0.4503(8)	C(43)	0.3551(5)	0.1660(15)	0.4897(10)
C(4)	0.4924(6)	0.3423(14)	0.5275(9)	C(44)	0.3409(6)	0.3082(16)	0.4820(10)
C(5)	0.4970(7)	0.4847(17)	0.5292(8)	C(45)	0.3458(5)	0.3727(16)	0.4039(10)
C(6)	0.5030(5)	0.5593(13)	0.4529(9)	C(46)	0.3645(5)	0.3002(15)	0.3303(10)
C(7)	0.5053(6)	0.4931(14)	0.3759(8)	C(51)	0.3735(8)	0.1397(19)	0.1592(12)
C(8)	0.5153(6)	0.5760(17)	0.2981(11)	C(52)	0.4001(6)	0.2243(17)	0.1029(11)
C(11)	0.6350(6)	0.1584(18)	0.1628(11)	C(53)	0.3700(7)	0.2867(18)	0.0368(11)
C(12)	0.6065(6)	0.2407(17)	0.1042(11)	C(54)	0.3144(6)	0.2641(17)	0.0263(11)
C(13)	0.6335(7)	0.3099(19)	0.0354(12)	C(55)	0.2872(6)	0.1741(19)	0.0790(12)
C(14)	0.6894(7)	0.2911(20)	0.0245(13)	C(56)	0.3156(6)	0.1108(17)	0.1474(11)
C(15)	0.7189(6)	0.2025(17)	0.0825(12)	C(61)	0.3775(4)	-0.1133(11)	0.2583(16)
C(16)	0.6916(5)	0.1405(16)	0.1495(11)	C(62)	0.4036(6)	-0.2188(16)	0.2127(10)
C(21)	0.6273(7)	0.1814(18)	0.3453(11)	C(63)	0.3789(6)	-0.3507(18)	0.2021(11)
C(22)	0.6252(5)	0.1234(15)	0.4241(10)	C(64)	0.3269(5)	-0.3703(15)	0.2374(11)
C(23)	0.6396(5)	0.2102(15)	0.4940(10)	C(65)	0.3008(5)	-0.2678(15)	0.2818(9)
C(24)	0.6567(7)	0.3459(19)	0.4797(12)	C(66)	0.3263(5)	-0.1343(15)	0.2912(10)
C(25)	0.6577(6)	0.4004(17)	0.3999(11)				
C(26)	0.6443(5)	0.3150(15)	0.3317(10)				

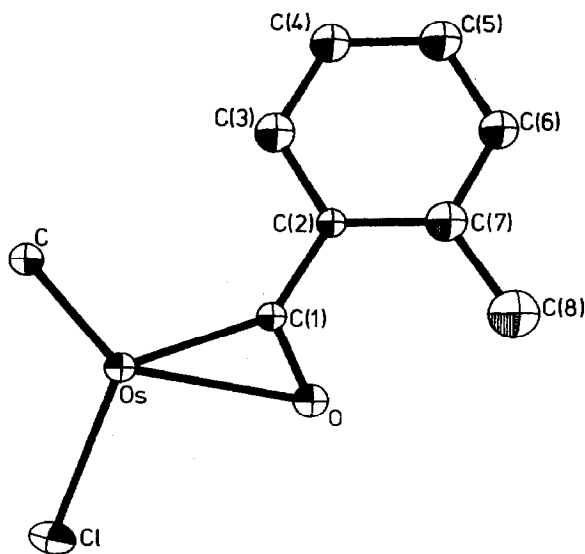
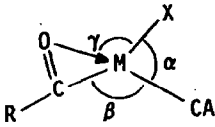
Fig. 2. View of  $\text{OsCl}(\eta^2\text{-C}[\text{O}]\text{-}o\text{-tolyl})(=\text{CH}_2)(\text{PPh}_3)_2$  (**2d**) along osmium–triphenylphosphine bond axis.

Table 5

In plane geometry of  $\eta^2$ -acyl complexes of osmium and ruthenium


M	A	X	R	Bond angles (°)			Ref.
				$\alpha$	$\beta$	$\gamma$	
Ru	O	I	<i>p</i> -tolyl	122.4(4)	104.5(6)	102.5(4)	27
Ru	O	I	Me	124(1)	98(2)	106.3(4)	27
Os	H <sub>2</sub>	Cl	<i>o</i> -tolyl	120.3(4)	109.8(5)	99.7(2)	This work

this fragment the plane of the methylene ligand is orthogonal to the plane defined by the Ru, Cl and H, and there is a high calculated barrier ( $\Delta G_{\text{rot}} \geq 13.6$  kcal/mol) for rotation around the ruthenium–methylene bond. Since the ground state of  $\text{RuHCl}(=\text{CH}_2)$  has a low spin state, there are empty axial orbitals that the triphenylphosphine ligands can use to form donor bonds to the metal. To generate a  $\eta^2$ -acyl complex analogous to **2a–2c** from  $\text{RuHCl}(=\text{CH}_2)(\text{PPh}_3)_2$  the  $\eta^2$ -acyl is required to substitute for the hydride, which in the GVB theory is regarded as forming covalent bonds to low valent metal centres. The applicability of these calculations to discussions of the geometry and dynamics of **2a–2c** thus depends largely upon the effect of such a substitution and additional theoretical results are needed before this question can be satisfactorily answered.

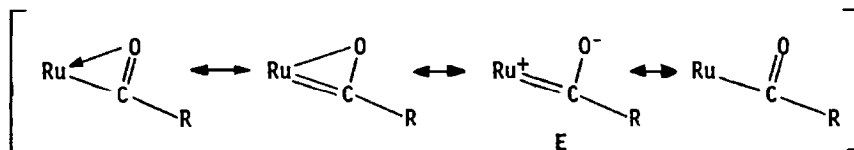
Table 6

Structural comparisons for osmium–carbon multiple bonds and other terminal methylene complexes

Complex	Os–C (Å)	Os–C–R (°)	Ref.
<i>Carbyne complexes</i>			
$\text{OsCl}_2(\text{NCS})(=\text{CR})(\text{PPh}_3)_2^a$	1.75(1)	169.5(9)	28
$[\text{OsCl}_2(=\text{CR})(\text{CN-}i{o}\text{-tolyl})(\text{PPh}_3)_2]\text{ClO}_4$	1.78(1)	174(1)	28
$\text{OsCl}(\text{CO})(\equiv\text{C-}i{o}\text{-tolyl})(\text{PPh}_3)_2$	1.77(2)	164(2)	29
<i>Carbene complexes</i>			
$\text{OsCl}(\eta^2\text{-C[O]-}i{o}\text{-tolyl})(=\text{CH}_2)(\text{PPh}_3)_2$	1.856(12)	–	This work
$\text{OsCl}_2(=\text{CHPh})(\text{CO})(\text{PPh}_3)_2$	1.94(1)	139(1)	28
$\text{Os}(=\text{C}=\text{C}(\text{CHMe})\text{C}_6\text{H}_4)(\text{CO})_2(\text{PPh}_3)_2$	1.90(1)	169(3)	31
$\text{OsCl}(\text{NO})(=\text{CH}_2)(\text{PPh}_3)_2$	1.92(1)	–	2
$\text{OsCl}(\text{NO})(=\text{CF}_2)(\text{PPh}_3)_2$	1.967(4)	131.4(10); 126.7(11)	46
<i>Other methylene complexes</i>			
$\text{Cp}_2\text{Ta}(=\text{CH}_2)(\text{CH}_3)$	2.026(10)	–	1
$[\text{Cp}^*\text{Re}(=\text{CH}_2)(\text{NO})\text{L}]\text{PF}_6$ (L = P(OPh) <sub>3</sub> )	1.898(18)	–	3
$\text{Ir}[\text{N}(\text{SiMe}_2\text{CH}_2\text{PPh}_2)_2](=\text{CH}_2)$	1.868(9)	–	4

<sup>a</sup> R = *p*-N,N-dimethylaminophenyl.

The  $\eta^2$ -acyl ligand is most often encountered in the chemistry of the early transition metals, and, as noted before, its appearance in an osmium complex is somewhat surprising. Aspects of the bonding in  $\eta^2$ -acyl complexes have recently been discussed in considerable detail [35]. One of the main features found in complexes containing this ligand is the variation in  $\Delta$ , the difference between the M–O and M–C bond lengths. Significantly,  $\Delta$  for the  $\eta^2$ -acyl ligands in complexes of the iron triad are much larger than those found in complexes containing the early transition metals. One interpretation of this trend is that it is due to the higher oxophilicity of the early transition metals. Other perspectives are that this trend is due to the increased carbenoid character of the acyl ligand or to an increase in the contribution of the  $\eta^1$ -acyl structures:



The carbon–osmium bond length for the  $\eta^2$ -acyl in **2d** is only slightly longer than the carbon–osmium bond lengths (Table 6) for carbene complexes. This suggests that the canonical form **E** may make a strong contribution to the bonding. However, the presence of an exceptionally long osmium–oxygen bond (in **2d** 2.423(9) Å while the range in related complexes is 2.026(4)–2.226(11) Å) suggests that the bonding may in fact be better represented by the canonical forms without osmium–oxygen bonds. Unfortunately the high esd's associated with the C–O bond length curtail any meaningful discussion of the response of this bond length to the resonance contributions above.

The range [28] for related osmium–chlorine bond lengths is 2.353(3)–2.507(4) Å and the Os–Cl bond in **2d** is a fairly short 2.401(3) Å. This is unexpected since many of the reactions that will be discussed for these species involve halide dissociation as an early or an initial step.

### Spectroscopic characterization of the terminal methylene complexes

Although the  $^1\text{H}$  NMR spectra of **2a–2d** have already been discussed in the preceding section a brief note of the  $^{13}\text{C}$  NMR spectra is merited. The metal bound carbon atoms of both the methylene and the acyl ligand have resonances that are shifted to very low fields. The resonance of the  $\eta^2$ -acyl ligand is particularly difficult to measure and this signal could only be discerned from the baseline noise for **2b** (a weak singlet  $\delta$ , 292.5 ppm and this is presumably the central peak of a triplet resonance) and for **2c** (a triplet  $\delta$ , 279.47 ppm with  $^3J(\text{CP})$  13.1 Hz).

In the infrared spectra of **2a–2d** there are two sets of bands that are diagnostic of the terminal methylene ligand in transition metal complexes. These are the symmetric and asymmetric C–H stretching modes near, 2900  $\text{cm}^{-1}$ , and bands that are probably due to a twist or a wagging deformation of the  $\text{CH}_2$  fragment, near 900  $\text{cm}^{-1}$ . Both sets of bands have medium to strong intensity and are easily identified in the spectra of **2a–2d**.

Unfortunately a metal–carbon stretching band cannot be assigned in this system because the expected region is obscured by strong triphenylphosphine bands. The calculated range [34] for this band in  $\text{RuHCl}(\text{CH}_2)$  is 740–800  $\text{cm}^{-1}$ .

There are three sets of intense bands which are associated with the presence of the  $\eta^2$ -acyl ligand. Typically these occur between 1550–1536, 1212–1168 and 916–885  $\text{cm}^{-1}$ . The high frequency band is almost certainly a combination of the carbon–oxygen stretching mode with other modes associated with the aryl ring. There is little variation in the frequency for this band and it is not very sensitive to the halide or the aryl group that is present. It may be significant that this band in the osmium complex, **2d**, is found at 1506  $\text{cm}^{-1}$  which is much lower than the values found for the ruthenium compounds. This can be attributed to the generally increased basicity of the osmium.

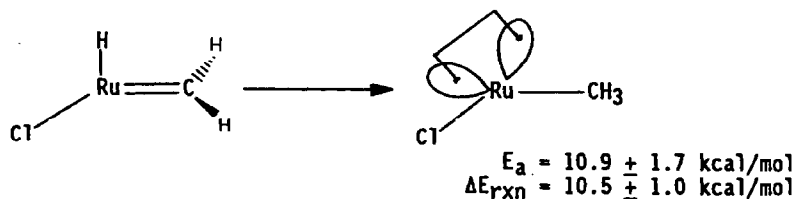
### Reactions of $\text{MCl}(\eta^2\text{-acyl})(=\text{CH}_2)(\text{PPh}_3)_2$

Unlike the reactions of the cationic  $d^6$  terminal methylene complexes outlined at the beginning of the chapter, nucleophiles do not readily add to the methylene ligand in **2a–2d**. Instead, the predominant reactivity pattern for these complexes involves initial loss or substitution of the chloride ligand. In this regard the chemistry of **2a–2d** resembles that of the coordinatively unsaturated precursors **1a–1d**. The chloride in these latter compounds is rapidly substituted by another halide or by chelating ligands such as formate or acetate [19,31].

### Decomposition of the terminal methylene complexes

It is often supposed that migration to a carbene ligand is much more facile than migration to a coordinated carbon monoxide. An important question in the chemistry of **2a–2d** is why the expected migration of the aryl group onto the methylene, to give a benzyl complex, is not observed? Stable examples of coordinatively saturated benzyl compounds are known [31] for both  $\text{Os}^{\text{II}}$  and  $\text{Ru}^{\text{II}}$  and these compounds are perfectly tractable species. We expect that a coordinatively unsaturated benzyl complex such as  $\text{RuCl}(\text{CH}_2\text{Ph})(\text{CO})(\text{PPh}_3)_2$  would be stable since the methyl, *trans*- $\beta$ -styryl and aryl analogues of **1a–1d** are known stable complexes. Yet they are not observed in the chemistry of **2a–2d**. In view of the migratory insertion reactions of **1** with CO and CNR which were described in the beginning of this section it is surprising that addition of a terminal  $\text{CH}_2$  ligand does not also exhibit this reactivity pattern. Migration of alkyl fragments onto methylene and alkylidene ligands is postulated as one of the key steps in the Fischer–Tropsch process and there are several reported examples of this reaction for cationic  $d^6$  complexes [12–14].

One reason why the migratory insertion of an aryl ligand to the methylene ligand in **2a–2d** is not found may be that there is a very high barrier for the migratory insertion of the phenyl to the methylene fragment. However, this seems unlikely in view of the experimental evidence mentioned above and also since recent calculations indicate that the barrier for hydride migration of methylene is only  $10.9 \pm 1.7$  kcal/mol and the calculated energy barriers for the related alkyl migrations are not much larger [34]:



An explanation which must also be considered is that the aryl and the methylene ligands may never be *cis* to one another. Some support for this idea is found in the structure in  $\text{Ru}(\text{CH}_2\text{OC}[\text{O}]\text{CH}_3)(\text{Ph})(\text{CO})(\text{PPh}_3)_2$  (**5a**) (see below). Reverse migration of the acyl phenyl onto the ruthenium here leaves it *trans* to the methylene in what is probably a kinetic product. If this reasoning also applies to **2a–2d** then the kinetic control of this migration can be attributed to the relative energies and configurations of the two transition states that would lead to the two possible products **F** and **G**.



The main objection to this explanation is that the relative positions of the aryl, carbonyl and *p*-tolylisocyanide ligands in the closely related compounds  $\text{RuCl}(\text{aryl})(\text{CN-}p\text{-tolyl})(\text{CO})(\text{PPh}_3)_2$  are known to change rapidly at 39°C.

Ethylene complexes are frequently the result of bimolecular decomposition of terminal methylene complexes. As in the case of  $\text{OsCl}(\text{NO})(=\text{CH}_2)(\text{PPh}_3)_2$ , there is no evidence that **2a–2d** decompose in this manner. For both of these bis(triphenylphosphine) complexes this is probably due to the steric bulk around the metal preventing the intermolecular coupling. While a stable ethylene adduct of  $\text{OsCl}(\text{NO})(\text{PPh}_3)_2$  is known, it would be surprising if such an adduct of  $\text{Os}^{\text{II}}$  would be stable. Thus, even if an ethylene complex such as “ $\text{RuCl}(\eta^2\text{-C}[\text{O}]\text{Ph})(\text{CH}_2=\text{CH}_2)(\text{PPh}_3)_2$ ” is formed, the ethylene could readily dissociate to give the coordinatively unsaturated complexes  $\text{MClR}(\text{CO})(\text{PPh}_3)_2$  (**1a–1d**). Spectroscopic studies of this reaction indicate that **1a–d** are not among the decomposition products of **2a–2d**.

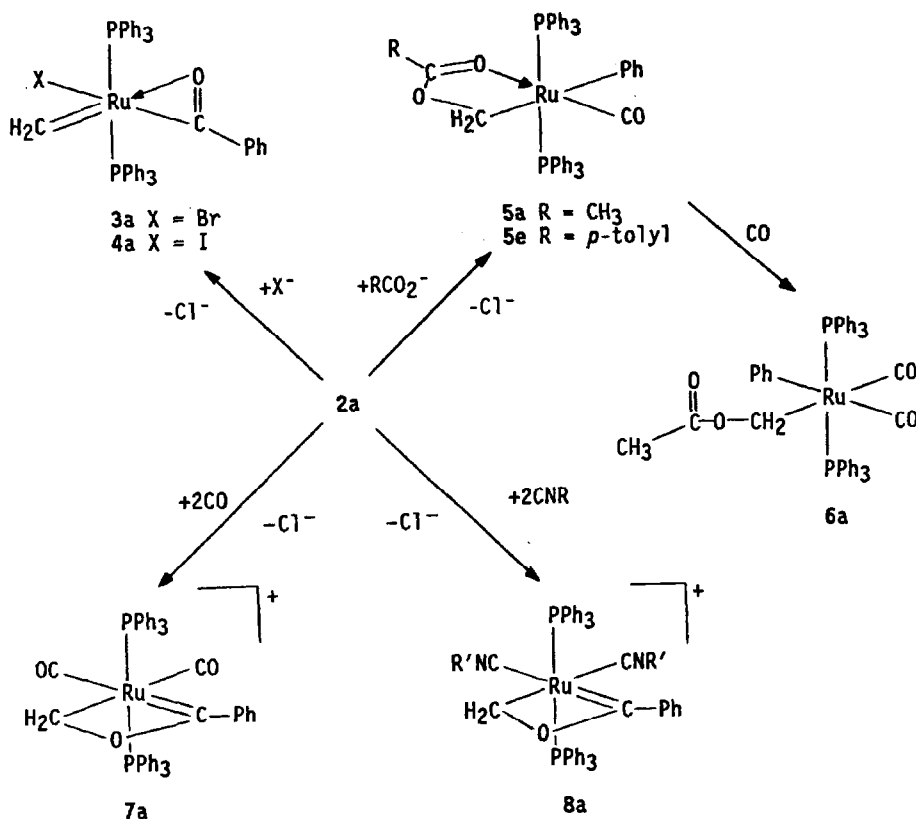
Thermolysis of **2d** in rigorously degassed THF at reflux for 1 h resulted in a brown solution which gave only ill-defined products which could not be purified by recrystallization.

Attempts to substitute a hydride into the coordination sphere of **2a** with lithium triethylborohydride resulted in poor returns ( $\approx 30\%$ ) of  $\text{RuH}_2(\text{CO})(\text{PPh}_3)_3$ .

### Halide exchange reactions of $\text{RuCl}(\eta^2\text{-C}[\text{O}]\text{Ph})(=\text{CH}_2)(\text{PPh}_3)_2$

Primarily because of synthetic convenience most of the exploratory reactions of **2a–2d** have been performed with the ruthenium phenyl derivative, **2a**. Scheme 1 depicts the important reactions of **2a**.

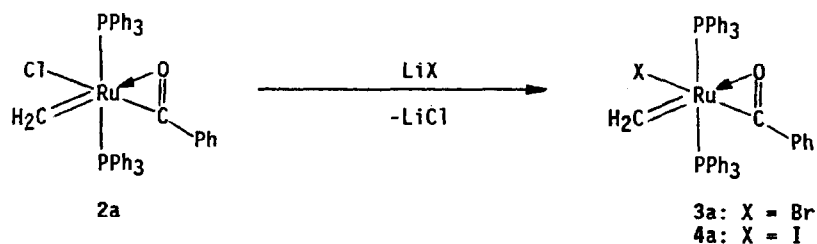
Recrystallization of the chloride complex **2a** from dichloromethane/ethanol in the presence of a 20 fold-excess of lithium bromide or lithium iodide results in rapid halide metathesis at room temperature. The resulting bromo, **3a**, and iodo, **4a**, derivatives are sparingly soluble orange crystalline solids that can be purified by additional recrystallization. The spectroscopic characteristics of the new methylene complexes **3a** and **4a** are almost identical to those of **2a**.



$\text{R}' = p\text{-tolyl}$

$\text{X} = \text{Br}, \text{I}$

Scheme 1. Reactions of  $\text{RuCl}(\eta^2\text{-C[O]Ph})(=\text{CH}_2)(\text{PPh}_3)_2$ .

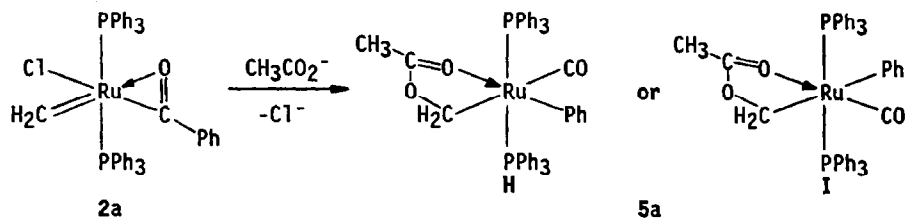


The facility of the halide exchange is surprising. The structural study of **2d** indicated that the osmium–chloride bond is relatively short. Also, the metal halide stretching frequencies, which range from  $300\text{--}282\text{ cm}^{-1}$  for **2a–2d**, do not suggest an unusually weak bond. Silver salts react rapidly at room temperature with **2a** to give a silver chloride precipitate and a black solution. If excess lithium chloride is then added to this solution there is no change in colour and starting material can not be recovered after removal of the silver chloride precipitate by filtration. Chloride abstraction clearly leads to rapid decomposition of what is probably a cationic terminal methylene complex.

The halide metathesis reaction of **2a** suggests that halide exchange for other anions may lead to new methylene compounds. Using the same conditions as employed above for the halide exchange reactions, intriguing products are recovered from the reaction of **2a** with either sodium acetate or sodium 4-methylbenzoate, and these results are described in the next section.

### Carboxylate addition across the metal–carbon double bond

Addition of an ethanol solution of sodium acetate to a solution of **2a** in dichloromethane causes rapid loss of the yellow-orange colour of **2a** and this is replaced within ten minutes by a very light yellow colour. The product from this reaction, **5a**, is recovered in 78% yield by crystallization from this solution and is characterized by strong bands at 1891, 1622 and 1364  $\text{cm}^{-1}$  in the IR spectrum. The first of these is due to a metal-bound terminal CO and the remaining two are due to a carboxylate group. The very large difference in the carboxylate stretching bands,  $\Delta 258 \text{ cm}^{-1}$ , clearly indicates that this ligand is not bound to the metal as a bidentate chelate. Furthermore, the  $^1\text{H}$  NMR spectrum for this product has a triplet,  $\delta 5.2$  ppm, which integrates for two protons, indicating that the methylene fragment has been retained in some form in this product. Many of the features of the IR spectrum, that is weak to moderately intense bands at 1564, 1072 and 1024  $\text{cm}^{-1}$ , are all indicative of a metal-bound phenyl group that could only arise from the acyl ligand reverting to an aryl and a carbon monoxide. There are two possible geometries for the product **5a**, but all of the spectroscopic evidence suggests that only one of these products is formed but does not differentiate between the isomers **H** and **I**:



On thermodynamic grounds the expected geometry for **5a** is the isomer **H** with two strong  $\sigma$ -donating ligands, the phenyl and the carbon of the  $\eta^2$ -acetatomethyl, mutually *cis* to one another.

### X-ray diffraction study of $\text{Ru}(\overline{\text{CH}_2\text{OC}(\text{O})\text{CH}_3})(\text{Ph})(\text{CO})(\text{PPh}_3)_2$ (**5a**)

The results of this study were very unexpected as the geometry of **5a** corresponds to the geometry **I**. Figure 3 depicts the full molecular structure of **5a** while bond lengths, bond angles and atomic positions are collected in Tables 7, 8 and 9 respectively.

Overall the structure of **5a** is that of an octahedral  $\text{Ru}^{\text{II}}$  complex. Although the carbonyl and oxygen of the  $\eta^2$ -acetatomethyl ligand are almost  $180^\circ$  apart, the angle between the metal bound aryl carbon and the methylene carbon is  $163.5(3)^\circ$ . The result of having the two strong  $\sigma$ -donor ligands *trans* to one another is seen in the ruthenium–carbon bond lengths ( $\text{Ru}-\text{CH}_2$  2.181(8) Å, and  $\text{Ru}-\text{C}_{\text{aryl}}$  2.160(8)



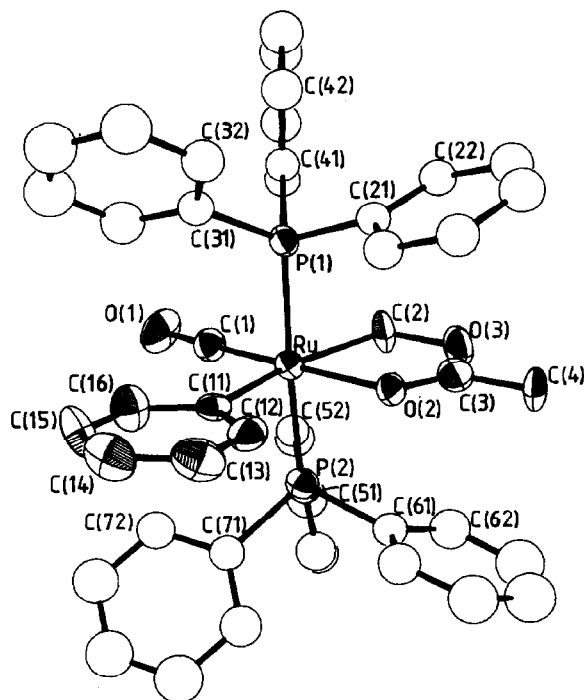


Fig. 3. Molecular structure of  $\text{Ru}(\text{CH}_2\text{OC}(\text{O})\text{CH}_3)(\text{Ph})(\text{CO})(\text{PPh}_3)_2$  (**5a**).

Table 7

Bond lengths for  $\text{Ru}(\text{CH}_2\text{OC}(\text{O})\text{CH}_3)(\text{Ph})(\text{CO})(\text{PPh}_3)_2$  (**5a**)<sup>a</sup>

*Bond lengths involving ruthenium (Å)*

P(1)–Ru	2.366(2)	C(2)–Ru	2.181(8)
P(2)–Ru	2.359(2)	O(2)–Ru	2.142(5)
C(1)–Ru	1.810(9)	C(11)–Ru	2.160(8)

*Bond lengths involving carbonyl, phenyl and  $\eta^2$ -acetomethyl ligands (Å)*

O(1)–C(1)	1.173(9)	C(12)–C(11)	1.386(11)
O(3)–C(2)	1.499(10)	C(16)–C(11)	1.397(11)
C(3)–O(2)	1.241(10)	C(13)–C(12)	1.393(12)
C(4)–C(3)	1.477(12)	C(14)–C(13)	1.363(13)
O(3)–C(3)	1.296(11)	C(15)–C(14)	1.371(13)
		C(16)–C(15)	1.353(12)

*Bond lengths involving triphenylphosphine ligands (Å)*

C(21)–P(1)	1.831(8)	C(51)–P(2)	1.829(8)
C(31)–P(1)	1.854(9)	C(61)–P(2)	1.814(9)
C(41)–P(1)	1.831(8)	C(71)–P(2)	1.844(9)

	<i>i</i>					
	2	3	4	5	6	7
C( <i>i</i> 1)–C( <i>i</i> 2)	1.40	1.38	1.38	1.38	1.39	1.35
C( <i>i</i> 1)–C( <i>i</i> 6)	1.37	1.37	1.40	1.41	1.39	1.38
C( <i>i</i> 2)–C( <i>i</i> 3)	1.41	1.41	1.39	1.39	1.43	1.42
C( <i>i</i> 3)–C( <i>i</i> 4)	1.33	1.36	1.35	1.37	1.32	1.37
C( <i>i</i> 4)–C( <i>i</i> 5)	1.37	1.36	1.37	1.38	1.33	1.34
C( <i>i</i> 5)–C( <i>i</i> 6)	1.38	1.40	1.40	1.39	1.40	1.41

<sup>a</sup> The esd for each carbon–carbon bond length within the phenyl rings of the triphenylphosphine ligands is 0.01 Å.

Table 8

Bond angles for  $\text{Ru}(\overline{\text{CH}_2\text{OC}[\text{O}]\text{CH}_3})\text{Ph}(\text{CO})(\text{PPh}_3)_2$  (**5a**)

<i>Angles at ruthenium (°)</i>			
C(1)–Ru–P(1)	90.8(2)	P(2)–Ru–P(1)	176.5(1)
C(1)–Ru–P(2)	92.2(2)	C(11)–Ru–P(1)	89.5(2)
C(2)–Ru–P(2)	89.3(3)	C(11)–Ru–P(2)	92.3(2)
C(2)–Ru–P(1)	88.1(3)	C(11)–Ru–C(1)	93.1(4)
C(2)–Ru–C(1)	103.3(4)	C(11)–Ru–C(2)	163.5(3)
O(2)–Ru–P(1)	89.0(1)	C(11)–Ru–O(2)	88.0(3)
O(2)–Ru–P(2)	88.1(1)		
O(2)–Ru–C(1)	178.9(3)		
O(2)–Ru–C(2)	75.5(3)		
<i>Angles involving carbonyl and phenyl ligands (°)</i>			
O(1)–C(1)–Ru	179.0(7)	C(14)–C(13)–C(12)	121.4(1.0)
C(12)–C(11)–Ru	119.4(7)	C(15)–C(14)–C(13)	117.2(9)
C(16)–C(11)–Ru	126.4(6)	C(16)–C(15)–C(14)	121.4(1.0)
C(16)–C(11)–C(12)	114.1(8)	C(15)–C(16)–C(11)	123.7(9)
C(13)–C(12)–C(11)	122.2(9)		
<i>Angles involving <math>\eta^2</math>-acetatomethyl ligand (°)</i>			
O(3)–C(2)–Ru	109.1(5)	O(3)–C(3)–O(2)	123.4(9)
C(3)–O(2)–Ru	116.3(6)	O(3)–C(3)–C(4)	115.0(9)
C(4)–C(3)–O(2)	121.6(1.0)	C(3)–O(3)–C(2)	115.6(7)
<i>Angles in triphenylphosphine ligands (°)<sup>a</sup></i>			
C(21)–P(1)–Ru	110.8(3)	C(51)–P(2)–Ru	118.7(3)
C(31)–P(1)–Ru	119.6(3)	C(61)–P(2)–Ru	111.6(3)
C(41)–P(1)–Ru	119.1(3)	C(71)–P(2)–Ru	118.7(3)
C(31)–P(1)–C(21)	103.8(4)	C(61)–P(2)–C(51)	103.3(4)
C(41)–P(1)–C(21)	103.0(4)	C(71)–P(2)–C(51)	97.5(4)
C(41)–P(1)–C(31)	98.2(4)	C(71)–P(2)–C(61)	104.9(4)

<sup>a</sup> Angles within triphenylphosphine phenyl rings not included.

Å). Comparable Ru–C( $\sigma$ -aryl) bond lengths have a range of 1.994(5)–2.16(8) Å with the long end of the range being due to the M–C bond in  $\text{RuH}(\text{naphthyl})(\text{dmpe})_2$  (dpme = bis(dimethylphosphino)ethane). The weakness of the bond in this latter complex is indicated by the very facile reductive elimination of naphthalene to give the reactive, coordinatively unsaturated, complex  $\text{Ru}(\text{dmpe})_2$  [36]. It can be seen in this comparison that both Ru–C bond lengths in **5a** are relatively long.

There are also some surprising trends in carbon–oxygen bond lengths within the  $\eta^2$ -acetatomethyl ligand. The two carbon–oxygen bond lengths to the trigonal planar carbon of the acetate are almost equivalent. Moreover, the carbon–oxygen bond length to the methylene carbon is relatively long, and it is longer than the sum of the covalent radii of these atoms [37]. This suggests that one way to view **5a** is that it is a weak adduct of a terminal methylene complex. The similarity of the carbon–oxygen bond lengths also indicates that there is a degree of electron delocalization between the C(3)–O(2) and the C(3)–O(3) bonds. It is possible then to consider that the bonding in this ligand is predominantly the result of two canonical forms:

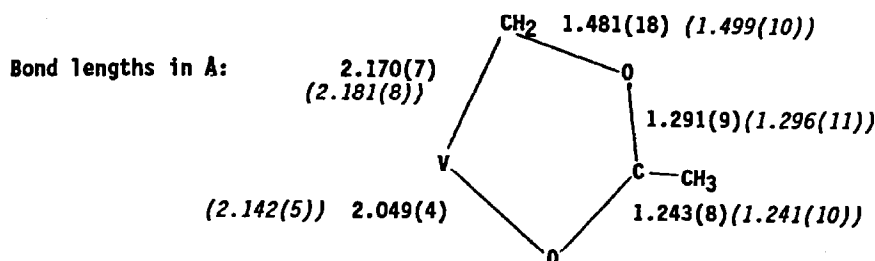


Table 9

Atomic positional parameters for  $\overline{\text{Ru}(\text{CH}_2\text{OC}[\text{O}]\text{CH}_3)\text{Ph}(\text{CO})(\text{PPh}_3)_2}$  (**5a**)

Atom	<i>x</i>	<i>y</i>	<i>z</i>	Atom	<i>x</i>	<i>y</i>	<i>z</i>
Ru	0.09239(5)	0.27209(3)	0.33890(5)	C(35)	0.2842(8)	0.0738(6)	0.2307(8)
P(1)	0.1873(1)	0.2714(1)	0.2402(1)	C(36)	0.2542(7)	0.1364(5)	0.2601(7)
P(2)	-0.0063(2)	0.2794(1)	0.4331(2)	C(41)	0.3121(6)	0.3056(4)	0.2886(6)
C(1)	0.1892(6)	0.2286(5)	0.4347(6)	C(42)	0.3671(7)	0.3074(5)	0.2309(7)
O(1)	0.2528(4)	0.2003(4)	0.4957(4)	C(43)	0.4620(7)	0.3334(5)	0.2647(7)
C(2)	0.1265(7)	0.3823(4)	0.3686(6)	C(44)	0.5021(8)	0.3571(5)	0.3563(7)
O(2)	-0.0205(4)	0.3254(3)	0.2264(4)	C(45)	0.4503(7)	0.3561(5)	0.4168(7)
C(3)	-0.0167(8)	0.3900(5)	0.2285(7)	C(46)	0.3546(6)	0.3309(4)	0.3826(6)
C(4)	-0.0907(8)	0.4329(5)	0.1554(8)	C(51)	0.0468(6)	0.3151(4)	0.5551(6)
O(3)	0.0508(5)	0.4250(3)	0.2938(5)	C(52)	0.1439(6)	0.3318(4)	0.5991(6)
C(11)	0.0258(6)	0.1752(4)	0.2739(5)	C(53)	0.1819(8)	0.3580(5)	0.6923(7)
C(12)	-0.0555(6)	0.1766(5)	0.1893(6)	C(54)	0.1213(8)	0.3675(6)	0.7428(8)
C(13)	-0.0976(7)	0.1160(5)	0.1401(7)	C(55)	0.0240(8)	0.3505(5)	0.7018(8)
C(14)	-0.0588(8)	0.0520(5)	0.1715(8)	C(56)	-0.0137(7)	0.3236(5)	0.6089(7)
C(15)	0.0195(9)	0.0494(5)	0.2570(8)	C(61)	-0.1122(6)	0.3342(4)	0.3762(6)
C(16)	0.0599(7)	0.1082(5)	0.3053(6)	C(62)	-0.1152(7)	0.4026(5)	0.4057(7)
C(21)	0.1296(6)	0.3242(4)	0.1318(6)	C(63)	-0.1986(8)	0.4439(6)	0.3540(8)
C(22)	0.1612(6)	0.3921(4)	0.1256(6)	C(64)	-0.2709(9)	0.4170(7)	0.2812(8)
C(23)	0.1110(7)	0.4314(5)	0.0420(6)	C(65)	-0.2700(8)	0.3521(6)	0.2500(8)
C(24)	0.0349(7)	0.4043(5)	-0.0287(7)	C(66)	-0.1898(7)	0.3095(5)	0.2971(7)
C(25)	0.0008(7)	0.3386(5)	-0.0232(6)	C(71)	-0.0555(6)	0.1984(5)	0.4641(6)
C(26)	0.0484(6)	0.2996(4)	0.0587(6)	C(72)	0.0085(7)	0.1464(5)	0.5020(6)
C(31)	0.2138(6)	0.1875(4)	0.1928(6)	C(73)	-0.0208(8)	0.0839(6)	0.5342(7)
C(32)	0.2063(6)	0.1787(5)	0.0983(6)	C(74)	-0.1176(8)	0.0775(6)	0.5220(8)
C(33)	0.2367(7)	0.1155(6)	0.0698(8)	C(75)	-0.1831(9)	0.1278(6)	0.4842(8)
C(34)	0.2734(8)	0.0644(6)	0.1367(8)	C(76)	-0.1516(7)	0.1899(5)	0.4539(7)

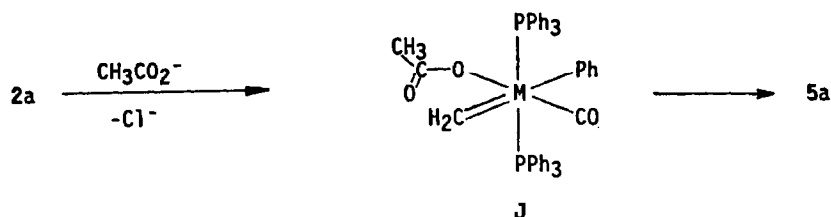
The dimensions of the acetatomethyl ligand are very similar to values reported recently [38] for the vanadium complex  $\text{Cp}_2\text{V}(\text{CH}_2\text{OC}[\text{O}]\text{CH}_3)$ . This complex, and its closely related phenyl derivative, are prepared by addition of acetyl chloride or benzoyl chloride to the  $\eta^2$ -formaldehyde complex  $\text{Cp}_2\text{V}(\eta^2\text{-CH}_2\text{O})$ . For comparison the corresponding bond lengths for  $\text{Cp}_2\text{V}(\text{CH}_2\text{OC}[\text{O}]\text{CH}_3)$  (bolded) and for **5a** (in italics) are:



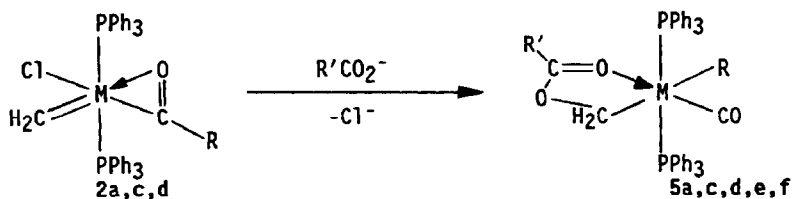
The most substantial difference between the two structures lies in the relative metal–oxygen bond lengths. However, both rings are essentially planar, with the largest out-of-plane deviations for **5a** being 0.007 Å for C(2) and 0.058 Å for the methylene carbon in  $\text{Cp}_2\text{V}(\text{CH}_2\text{OC}[\text{O}]\text{CH}_3)$ .

Three separate steps are involved in the transformation of **2a** to **5a**: (1) Substitution of chloride for acetate. (2) Migration of the phenyl group back to the metal. (3) Additional of the acetate group to the methylene ligand.

It would be surprising if this reaction began with nucleophilic attack by the acetate on the methylene. Better nucleophiles do not attack the methylene carbon, and thus it is unlikely that acetate would initially attack here. The scope of this reaction is very limited, and other simple carboxylates such as formate and trifluoroacetate, do not react in this manner with **2a**. In view of the lability of the chloride in **2a**, the most likely first step in this reaction is anion substitution. The sequence of events after this must remain uncertain, but an attractive theory is that nucleophilic addition to the methylene takes place after migration of the phenyl to the metal to give an intermediate **J**. In **J** the competition for  $\pi$ -electron density between the carbon monoxide and methylene ligands is bound to leave the methylene carbon more susceptible to nucleophilic attack, which in this case leads to **5a**:



Four other addition products have been characterized in the course of this research and these correspond to the addition of acetate to **2c** and **2d**, and 4-methylbenzoate to **2a** and **2c**:



**5a**: M = Ru, R = Ph, R' = Me

**5e**: M = Ru, R = Ph, R' = *p*-tolyl

**5c**: M = Ru, R = *p*-tolyl, R' = Me

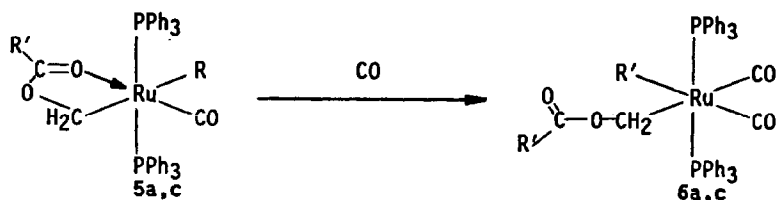
**5f**: M = Ru, R = *p*-tolyl, R' = *p*-tolyl

**5d**: M = Os, R = *o*-tolyl, R' = Me

The ruthenium complexes **5c**, **5e**, **5f** are similar in many respects to **5a**. But the osmium complex **5d** is less stable and decomposes during recrystallization in the absence of acetate. All of the complexes **5a-f** are unstable in solution, and solutions of these species discolour within several hours at room temperature. The nature of these decomposition products is not certain and attempts to follow this reaction by  $^1\text{H}$  NMR do not indicate the presence of the other possible isomer of **5a**, **I**.

### Reactions of acetate addition products

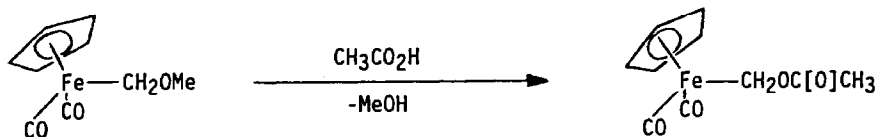
Both **5a** and **5c** react rapidly with carbon monoxide to give dicarbonyl complexes with a  $\eta^1$ -carboxymethyl ligand, **6a**, **6c**:



a: R = Ph, R' = CH<sub>3</sub>    b: R = R' = *p*-tolyl

This reaction again demonstrates the flexibility of the coordination sphere at the ruthenium since the product now has the aryl and  $\eta^1$ -carboxymethyl ligands *cis*. The above geometry can be firmly assigned to **6a,6c** on the basis of the position and presence of two strong carbonyl stretching bands in the IR spectrum for both of these compounds. The carboxylate stretching bands for **6a**, 1717 and 1366 cm<sup>-1</sup>, have a much greater difference than is found for **5a**. Either in solution or in the solid state, **6a,6c** are much more stable than **5a,5c** as there is no evidence for decomposition of **6a,6c** after standing for 24 hours at room temperature.

Carboxymethyl compounds are rather unusual and one of the few reported examples of this type of complex results from treating a methoxymethyl complex with acetic acid [39]:



This type of reactivity suggests that addition of acid to **6a,6c**, or indeed **5a–5e**, may also generate cationic methylene complexes that are capable of either anion exchange or aryl migration to methylene. In situ NMR experiments indicate that acid reacts rapidly with both **6a** and **5a** but the products from these reactions do not include benzyl complexes.

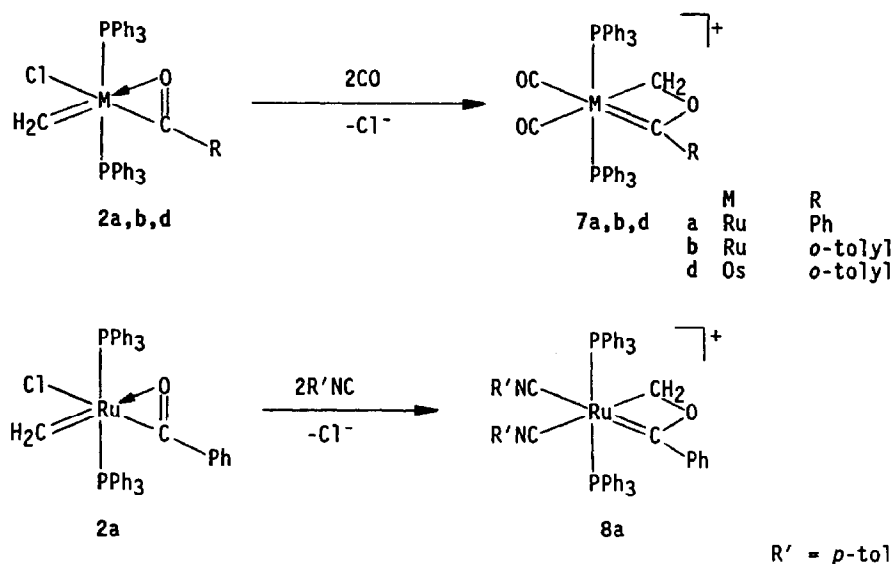
#### Addition of carbon monoxide and isocyanides to **2a**: formation of metallaoxetenes

The most interesting reactions of **2** are with the  $\pi$ -acid ligands carbon monoxide and *p*-tolylisocyanide. In these cases two molecules of CO or *p*-tolylisocyanide are incorporated into the molecule, with loss of chloride, and the oxygen of the acyl ligand adds to the methylene carbon to give the metallaoxetenes **7a,7b,7d** and **8a**: The cationic products **7a,7b,7d** and **8a** are readily isolated as perchlorate salts and are remarkably air-stable crystalline solids.

#### X-ray diffraction study of $[\text{Ru}(\text{C}(\text{Ph})\text{OCH}_2)(\text{CN-}i\text{p-tolyl})_2(\text{PPh}_3)_2]\text{ClO}_4$ (**8a**)

This study confirmed the proposed structure of **8a**, and, by analogy, that of **7a,7c,7d**. The molecular structure of **8a** is depicted in Fig. 4 while bond length, bond angle and atomic positional data are collected in Tables 10, 11 and 12 respectively.

There are four Ru–C bonds and these allow for an interesting set of internal comparisons. The longest of these bonds is that of the methylene carbon (Ru–C(11) 2.164(6) Å) which is almost as long as the Ru–CH<sub>2</sub> bond in  $\text{Ru}(\text{CH}_2\text{OC}(\text{O})\text{CH}_3)(\text{Ph})(\text{CO})(\text{PPh}_3)_2$  (**5a**). The shortest Ru–C bond lengths are to the two isocyanide ligands, and although the very small difference between the Ru–C(21) and Ru–C(31)



bond is not significant it is worth noting that there is a large difference (7 Hz) in the carbon-phosphorus coupling constants for these two ligands (Table 14).

The metallaoxetene ring is planar, with the largest out-of-plane displacement being 0.002 Å by the oxygen atom. This planarity is not surprising since oxetanes [40] are planar and calculations for oxetenes [41] suggest that these unstable species are also planar. The trends of the bond lengths within this ring are significant and

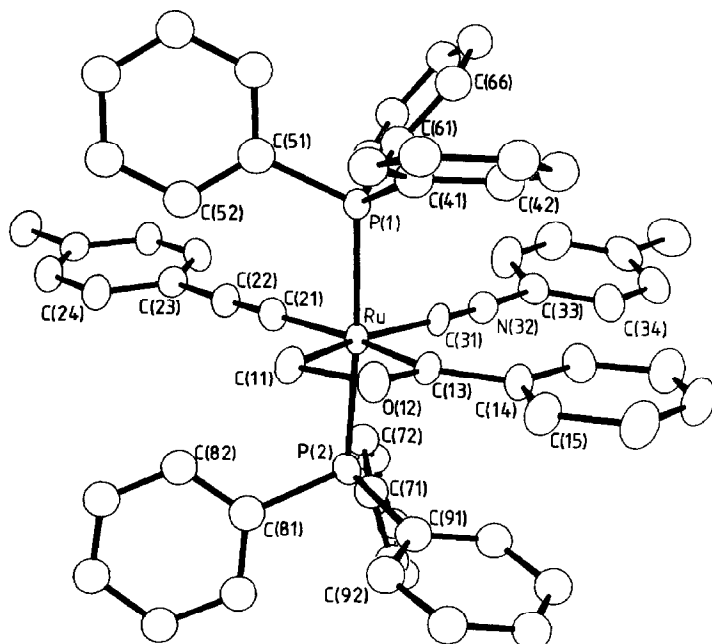


Fig. 4. Molecular structure of  $\text{Ru}(\text{=C}(\text{Ph})\text{OCH}_2)(\text{CN-}p\text{-tolyl})_2(\text{PPh}_3)_2\text{ClO}_4$  (**8a**).

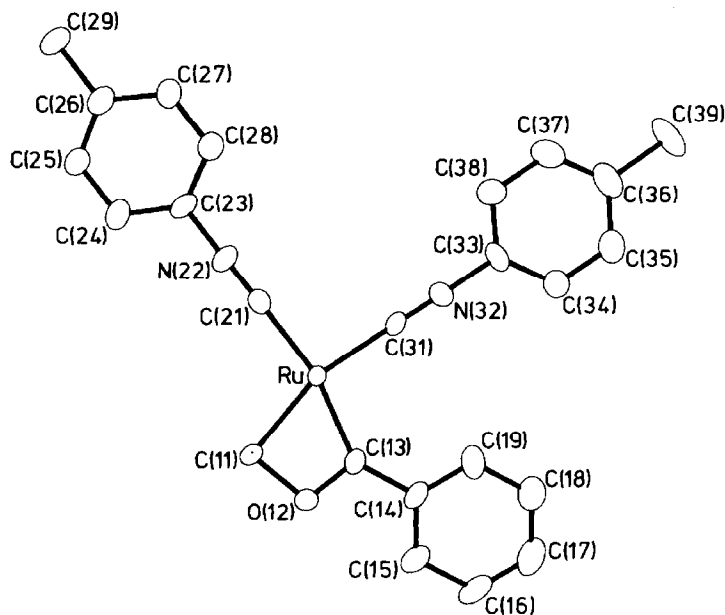
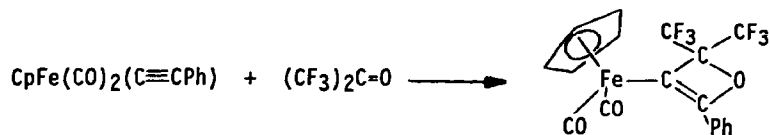


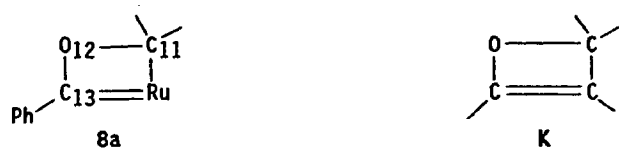
Fig. 5. View of  $[\text{Ru}(\text{=C}(\text{Ph})\text{OCH}_2)(\text{CN-}p\text{-tolyl})_2(\text{PPh}_3)_2]\text{ClO}_4$  (**8a**) along ruthenium–triphenylphosphine bond axis.

there is a large difference in the two carbon–oxygen bond lengths ( $\text{C}(11)\text{--O}(12)$  1.508(8) and  $\text{C}(13)\text{--O}(12)$  1.313(8) Å). Figure 5, a view of **8a** from along the metal–triphenylphosphine axis, clearly shows this difference in bond lengths. Heteroatom carbene complexes [42] often have short  $\text{C}(\text{carbene})\text{--element}$  bond lengths due to the  $\pi$ -interaction of the element lone pairs with the carbene  $\pi$ -orbital. Although this interaction can account for the contraction of  $\text{C}(13)\text{--O}(12)$  bond it does not rationalize the increase of the  $\text{C}(11)\text{--O}(12)$  bond length.

A search of the Cambridge crystallographic data files indicated that the metalated structural unit found in **8a** is unprecedented. There is however, an example of the stabilization of an oxetene in the coordination sphere of an iron complex [43]:



The parent oxetenes, **K**, are thermally unstable compounds that are often postulated as reactive intermediates [44]. Ab initio calculations predict that the  $\text{C}(sp^3)\text{--O}$  bond



length is the longest in this molecule, and it is often found that this bond is ruptured by strong acids or photochemical activation [41,44]. It is noteworthy that the corresponding bond in **8a** ( $\text{C}(12)\text{--O}(11)$ ) is also the longest of the two  $\text{C--O}$  bonds. The metallaoxetenes **7a**, **7b**, **7d** and **8a** do not exhibit any propensity for either ring

Table 10

Bond lengths for  $[\text{Ru}(\overline{=\text{C}(\text{Ph})\text{OCH}_2})(\text{CN-}p\text{-tolyl})_2(\text{PPh}_3)_2]\text{ClO}_4 \cdot \text{CH}_2\text{Cl}_2$  (**8a**)<sup>a</sup>

Bond lengths involving ruthenium (Å)						
P(1)–Ru	2.370(2)	C(13)–Ru	2.006(7)			
P(2)–Ru	2.366(2)	C(21)–Ru	1.998(7)			
C(11)–Ru	2.164(6)	C(31)–Ru	2.001(6)			
Bond lengths within the metallaoxetene fragment (Å)						
O(12)–C(11)	1.508(8)	C(15)–C(16)	1.436(12)			
O(12)–C(13)	1.313(8)	C(16)–C(17)	1.377(12)			
C(13)–C(14)	1.481(9)	C(17)–C(18)	1.390(13)			
C(14)–C(15)	1.411(10)	C(18)–C(19)	1.398(11)			
C(14)–C(19)	1.392(10)					
Bond lengths within the isocyanide ligands (Å)						
C(21)–N(22)	1.166(9)	C(31)–N(32)	1.135(9)			
C(23)–N(22)	1.404(9)	C(33)–N(32)	1.411(9)			
C(23)–C(24)	1.402(10)	C(33)–C(34)	1.394(10)			
C(23)–C(28)	1.385(10)	C(33)–C(38)	1.399(10)			
C(24)–C(25)	1.393(10)	C(34)–C(35)	1.390(11)			
C(25)–C(26)	1.381(10)	C(35)–C(36)	1.429(11)			
C(26)–C(27)	1.415(10)	C(36)–C(37)	1.377(12)			
C(26)–C(29)	1.530(10)	C(36)–C(39)	1.521(12)			
C(27)–C(28)	1.389(10)	C(37)–C(38)	1.396(11)			
Bond lengths within the triphenylphosphine ligands (Å)						
C(41)–P(1)	1.818(7)	C(71)–P(2)	1.838(7)			
C(51)–P(1)	1.834(7)	C(81)–P(2)	1.845(7)			
C(61)–P(1)	1.817(6)	C(91)–P(2)	1.824(6)			
<i>i</i>						
	4	5	6	7	8	9
C( <i>i</i> 1)–C( <i>i</i> 2)	1.40	1.41	1.40	1.41	1.39	1.42
C( <i>i</i> 1)–C( <i>i</i> 6)	1.40	1.40	1.40	1.40	1.42	1.39
C( <i>i</i> 2)–C( <i>i</i> 3)	1.39	1.41	1.40	1.42	1.40	1.42
C( <i>i</i> 3)–C( <i>i</i> 4)	1.39	1.38	1.40	1.38	1.35*	1.37
C( <i>i</i> 4)–C( <i>i</i> 5)	1.39	1.39	1.37	1.39	1.43*	1.39
C( <i>i</i> 5)–C( <i>i</i> 6)	1.41	1.40	1.41	1.40	1.42	1.40

<sup>a</sup> The csd for each carbon–carbon bond length within the phenyl rings of the triphenylphosphine ligands is 0.01 Å, except for those marked with (\*) where it is 0.02 Å.

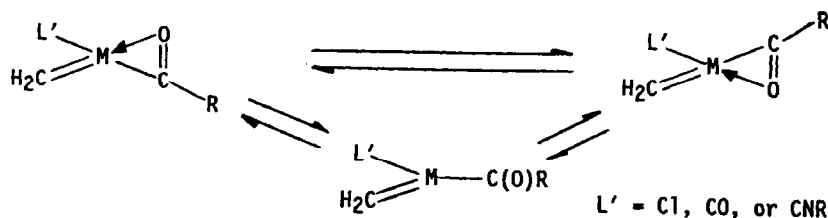
opening or other decomposition reactions. These species do not react with acid and attempts to add hydride have also failed to give any reaction.

### Possible significance and the mechanism for the formation of the metallaoxetenes

There are two features of this reaction which must be rationalized: (1) The “flip” or “twist” of the  $\eta^2$ -acyl ligand in order for the oxygen to be *cis* to the methylene ligand. (2) Combination of the oxygen of the acyl ligand and methylene ligand.

The twist of the  $\eta^2$ -acyl ligand is required since the structure of **2d** indicates that the oxygen of the acyl is *trans* to the methylene carbon. This twist may be quite facile since there is a possible *dihapto*  $\rightleftharpoons$  *monohapto* interconversion:





Alternatively, rotation around the metal-acyl bond would also transpose the relative positions of the carbon and the oxygen. It is not clear if this rotation occurs before or after chloride substitution, and thus  $L'$  may be Cl, CO, or CNR.

Table 11

Bond angles for  $[\text{Ru}(\text{=C}(\text{Ph})\text{OCH}_2)(\text{CN-}p\text{-tolyl})_2(\text{PPh}_3)_2]\text{ClO}_4 \cdot \text{CH}_2\text{Cl}_2$  (**8a**)

Angles at ruthenium ( $^\circ$ )			
C(11)–Ru–P(1)	87.5(2)	P(2)–Ru–P(1)	174.8(1)
C(11)–Ru–P(2)	87.6(2)	C(13)–Ru–P(1)	90.9(2)
C(11)–Ru–C(13)	62.7(2)	C(13)–Ru–P(2)	88.5(2)
C(11)–Ru–C(21)	104.2(3)	C(13)–Ru–C(21)	166.9(3)
C(11)–Ru–C(31)	163.4(3)	C(13)–Ru–C(31)	100.8(3)
C(21)–Ru–P(1)	88.2(2)	C(31)–Ru–P(1)	91.2(2)
C(21)–Ru–P(2)	91.2(2)	C(31)–Ru–P(2)	94.0(2)
C(21)–Ru–C(31)	92.2(3)		
Angles involving the metallaoxetene ligand ( $^\circ$ )			
O(12)–C(11)–Ru	91.5(4)	C(15)–C(14)–C(19)	121.7(7)
C(11)–O(12)–C(13)	100.6(5)	C(14)–C(15)–C(16)	117.4(7)
O(12)–C(13)–Ru	105.2(4)	C(15)–C(16)–C(17)	119.6(8)
C(14)–C(13)–Ru	143.2(5)	C(16)–C(17)–C(18)	122.4(8)
O(12)–C(13)–C(14)	111.6(6)	C(17)–C(18)–C(19)	119.0(8)
C(13)–C(14)–C(15)	119.3(6)	C(18)–C(19)–C(14)	119.9(7)
C(13)–C(14)–C(19)	118.9(6)		
Angles involving the <i>p</i> -tolylisocyanide ligands ( $^\circ$ )			
N(22)–C(21)–Ru	178.3(6)	N(32)–C(31)–Ru	177.5(6)
C(23)–N(22)–C(21)	177.8(7)	C(33)–N(32)–C(31)	176.6(7)
C(24)–C(23)–N(22)	118.8(6)	C(34)–C(33)–N(32)	119.3(6)
C(28)–C(23)–N(22)	118.7(6)	C(38)–C(33)–N(32)	118.7(6)
C(24)–C(23)–C(28)	122.5(6)	C(34)–C(33)–C(38)	121.9(7)
C(23)–C(24)–C(25)	117.9(7)	C(33)–C(34)–C(35)	118.9(7)
C(24)–C(25)–C(26)	121.8(7)	C(34)–C(35)–C(36)	119.8(7)
C(25)–C(26)–C(27)	118.3(6)	C(35)–C(36)–C(37)	119.9(7)
C(25)–C(26)–C(29)	121.2(7)	C(35)–C(36)–C(39)	120.3(7)
C(27)–C(26)–C(29)	120.5(6)	C(37)–C(36)–C(39)	119.8(7)
C(26)–C(27)–C(28)	121.6(6)	C(36)–C(37)–C(38)	120.9(7)
C(27)–C(28)–C(23)	117.8(6)	C(37)–C(38)–C(33)	118.6(7)
Angles in the triphenylphosphine ligands ( $^\circ$ ) <sup>a</sup>			
C(41)–P(1)–Ru	112.6(2)	C(71)–P(2)–Ru	118.2(2)
C(51)–P(1)–Ru	117.3(2)	C(81)–P(2)–Ru	115.6(2)
C(61)–P(1)–Ru	115.7(2)	C(91)–P(2)–Ru	112.6(2)
C(51)–P(1)–C(41)	102.1(3)	C(81)–P(2)–C(71)	101.8(3)
C(61)–P(1)–C(41)	106.9(3)	C(91)–P(2)–C(71)	102.4(3)
C(61)–P(1)–C(51)	100.7(3)	C(91)–P(2)–C(81)	104.4(3)

<sup>a</sup> Angles within triphenylphosphine phenyl rings not included.

Table 12. Atomic positional parameters for  $[\text{Ru}(\text{C}(\text{Ph})\text{OCH}_2)(\text{CN-}i\text{-tolyl})_2(\text{PPh}_3)_2]\text{ClO}_4 \cdot \text{CH}_2\text{Cl}_2$  (**8a**)

Atom	x	y	z	Atom	x	y	z
Ru	0.05667(9)	0.19874(6)	0.21853(7)	C(55)	0.0557(5)	0.4072(4)	0.0471(4)
P(1)	0.0695(1)	0.2001(1)	0.0927(1)	C(56)	0.0577(4)	0.3449(3)	0.0844(4)
P(2)	0.0513(1)	0.2072(1)	0.3448(1)	C(61)	-0.0160(4)	0.1514(3)	0.0359(4)
O(12)	0.2366(3)	0.2109(2)	0.2456(3)	C(62)	-0.1066(5)	0.1630(4)	0.0459(4)
C(11)	0.1700(4)	0.2691(3)	0.2325(4)	C(63)	-0.1775(5)	0.1313(4)	0.0018(5)
C(13)	0.1811(4)	0.1583(3)	0.2399(4)	C(64)	-0.1563(6)	0.0870(4)	-0.0531(4)
C(14)	0.2307(5)	0.0927(3)	0.2516(4)	C(65)	-0.0682(6)	0.0742(4)	-0.0623(5)
C(15)	0.3253(5)	0.0937(4)	0.2716(4)	C(66)	0.0036(5)	0.1065(4)	-0.0184(4)
C(16)	0.3711(6)	0.0288(5)	0.2797(5)	C(71)	-0.0473(4)	0.1709(3)	0.3818(4)
C(17)	0.3221(6)	-0.0307(4)	0.2674(5)	C(72)	-0.1306(4)	0.1670(3)	0.3373(4)
C(18)	0.2289(6)	-0.0308(4)	0.2473(5)	C(73)	-0.2085(5)	0.1443(4)	0.3676(4)
C(19)	0.1828(6)	0.0316(4)	0.2407(4)	C(74)	-0.2019(5)	0.1261(4)	0.4397(4)
N(22)	-0.1138(4)	0.2957(3)	0.1854(3)	C(75)	-0.1194(5)	0.1296(4)	0.4832(4)
C(21)	-0.0518(5)	0.2594(3)	0.1982(3)	C(76)	-0.0418(5)	0.1525(4)	0.4548(4)
C(23)	-0.1893(4)	0.3383(4)	0.1674(4)	C(81)	0.0548(4)	0.2949(4)	0.3819(4)
C(24)	-0.1785(5)	0.4092(4)	0.1755(4)	C(82)	0.0363(5)	0.3509(4)	0.3366(5)
C(25)	-0.2541(5)	0.4505(4)	0.1570(4)	C(83)	0.0331(6)	0.4177(4)	0.3637(6)
C(26)	-0.3376(5)	0.4233(4)	0.1311(4)	C(84)	0.0470(6)	0.4286(5)	0.4356(7)
C(27)	-0.3456(5)	0.3513(4)	0.1249(4)	C(85)	0.0674(6)	0.3728(5)	0.4845(6)
C(28)	-0.2717(5)	0.3084(4)	0.1423(4)	C(86)	0.0701(5)	0.3049(4)	0.4580(4)
C(29)	-0.4199(5)	0.4694(4)	0.1107(4)	C(91)	0.1458(4)	0.1635(4)	0.3976(3)
C(31)	-0.0191(4)	0.1140(3)	0.2076(4)	C(92)	0.2267(5)	0.1999(4)	0.4206(4)
N(32)	-0.0609(4)	0.0654(3)	0.1992(3)	C(93)	0.3004(5)	0.1618(5)	0.4560(4)
C(33)	-0.1143(5)	0.0062(3)	0.1843(4)	C(94)	0.2956(5)	0.0927(5)	0.4674(4)
C(34)	-0.0759(5)	-0.0580(4)	0.1998(4)	C(95)	0.2162(5)	0.0576(4)	0.4434(4)
C(35)	-0.1293(6)	-0.1160(4)	0.1853(4)	C(96)	0.1415(5)	0.0933(4)	0.4088(4)
C(36)	-0.2214(6)	-0.1089(4)	0.1538(4)	C(A)	0.4270(6)	0.2730(5)	0.2273(5)
C(37)	-0.2571(5)	-0.0448(4)	0.1385(5)	Cl(A1)	-0.0873(2)	0.2077(1)	-0.1825(1)
C(38)	-0.2044(5)	0.0138(4)	0.1534(5)	Cl(A2)	-0.0997(2)	0.1570(1)	-0.3279(1)
C(39)	-0.2809(6)	-0.1719(5)	0.1385(5)	Cl(B1)	0.6013	0.1394	0.1907
C(41)	0.1792(4)	0.1698(3)	0.0725(3)	Cl(C1)	0.5839	0.1055	0.2146
N(42)	0.1991(5)	0.0998(3)	0.0769(4)	O(B1)	0.5747	0.0682	0.1556
C(43)	0.2862(5)	0.0763(4)	0.0703(4)	O(B2)	0.5572	0.1908	0.1395
C(44)	0.3555(5)	0.1222(4)	0.0614(4)	O(B3)	0.6921	0.1481	0.1950
C(45)	0.3356(5)	0.1916(4)	0.0564(4)	O(B4)	0.5692	0.1479	0.2596
C(46)	0.2478(5)	0.2167(4)	0.0625(4)	O(C1)	0.6061	0.0624	0.2719
C(51)	0.0603(4)	0.2833(3)	0.0468(4)	O(C2)	0.5102	0.1442	0.2213
C(52)	0.0569(4)	0.2843(4)	-0.0295(4)	O(C3)	0.5748	0.0682	0.1556
C(53)	0.0529(5)	0.3474(4)	-0.0661(4)	O(C4)	0.6661	0.1455	0.2173
C(54)	0.0529(5)	0.4076(4)	-0.0278(5)				

Carbonylation of the osmium terminal methylene complex **2d** produces a second complex in addition to **7d**. This second, neutral, bright yellow product is formulated on the basis of spectroscopy and microanalysis as  $\text{Os}(\text{C}(\text{R})\text{OCH}_2)\text{Cl}(\text{CO})(\text{PPh}_3)_2$  (**9**):

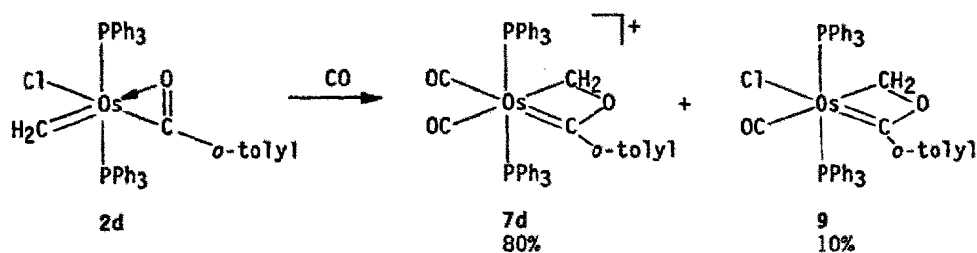


Table 13

Infrared data for new compounds <sup>a</sup>

Compound	$\nu(\text{C-O})$ <sup>b</sup>	Other bands
RuCl( $\eta^2\text{-C[O]Ph}(\text{=CH}_2)(\text{PPh}_3)_2$ ) (2a)		2930w, 2893w, $\nu(\text{C-H})$ 1542m, 1207s, 885s, (acyl) 931w, 915w, $\rho(\text{CH}_2)$ 283m, $\nu(\text{Ru-Cl})$
RuCl( $\eta^2\text{-C[O]-}o\text{-tolyl}(\text{=CH}_2)(\text{PPh}_3)_2$ ) (2b)		2903w, $\nu(\text{C-H})$ 1540m, 1187s, 892s, (acyl) 930m, 917m, $\rho(\text{CH}_2)$ 778m, ( <i>o</i> -tolyl) 300m, $\nu(\text{Ru-Cl})$
RuCl( $\eta^2\text{-C[O]-}p\text{-tolyl}(\text{=CH}_2)(\text{PPh}_3)_2$ ) (2c)		2903w, 2856w, $\nu(\text{C-H})$ 1603m, ( <i>p</i> -tolyl) 1536m, 1168s, 900s, (acyl) 938m, 910w, $\rho(\text{CH}_2)$ 790m, ( <i>p</i> -tolyl) 285m, $\nu(\text{Ru-Cl})$
OsCl( $\eta^2\text{-C[O]-}o\text{-tolyl}(\text{=CH}_2)(\text{PPh}_3)_2$ ) (2d)		2893w, 2810w, $\nu(\text{C-H})$ 1506w, ( <i>o</i> -tolyl) 1506m, 1196s, 904s, (acyl) 938m, 918m, $\rho(\text{CH}_2)$ 783m, ( <i>o</i> -tolyl) 292m, $\nu(\text{Os-Cl})$
RuBr( $\eta^2\text{-C[O]Ph}(\text{=CH}_2)(\text{PPh}_3)_2$ ) (3a)		2923m, $\nu(\text{C-H})$ 1543m, 1207s, 886s, (acyl) 932m, 913w, $\rho(\text{CH}_2)$
RuI( $\eta^2\text{-C[O]Ph}(\text{=CH}_2)(\text{PPh}_3)_2$ ) (4a)		2920m, 2881m, $\nu(\text{C-H})$ 1540m, 1202s, 898s, (acyl) 940w, $\rho(\text{CH}_2)$
Ru(CH <sub>2</sub> OC[O]Me)(Ph)(CO)(PPh <sub>3</sub> ) <sub>2</sub> (5a)	1891 1845cs	1622s, 1364m, 1184m, 802s, ( $\eta^2\text{-CH}_2\text{OC[O]CH}_3$ ) 1564m, 1072w, 1024m, 906m, (phenyl)
Ru(CH <sub>2</sub> OC[O]Me)( <i>p</i> -tolyl)(CO)(PPh <sub>3</sub> ) <sub>2</sub> (5c)	1888	1630s, 1397w, 1183w, ( $\eta^2\text{-CH}_2\text{OC[O]CH}_3$ ) 1013w, 950w, 799s
Os(CH <sub>2</sub> OC[O]Me)( <i>o</i> -tolyl)(CO)(PPh <sub>3</sub> ) <sub>2</sub> (5d)	1897 1875cs	1610m, 1472m, 1407w, 800m, ( $\eta^2\text{-CH}_2\text{OC[O]CH}_3$ )
Ru(CH <sub>2</sub> OC[O]- <i>p</i> -tolyl)(Ph)(CO)(PPh <sub>3</sub> ) <sub>2</sub> (5e)	1887	1610m, 1379s, 1181m, ( $\eta^2\text{-CH}_2\text{OC[O]R}$ ) 1564m, 791w, ( <i>p</i> -tolyl)
Ru(CH <sub>2</sub> OC[O]- <i>p</i> -tolyl)( <i>p</i> -tolyl)(CO)(PPh <sub>3</sub> ) <sub>2</sub> (5f)	1886	1611s, 1384s, 1180s, ( $\eta^2\text{-CH}_2\text{OC[O]R}$ ) 1115m, 1014, 797m, 786w, ( <i>p</i> -tolyl)
Ru(CH <sub>2</sub> O <sub>2</sub> CCH <sub>3</sub> )(Ph)(CO) <sub>2</sub> (PPh <sub>3</sub> ) <sub>2</sub> (6a)	2017 1952	1717s, 1366m, 1273s, 1205s, 941, 863, (CH <sub>2</sub> OC[O]CH <sub>3</sub> ) 1013w, 1003w, (phenyl)
Ru(CH <sub>2</sub> O <sub>2</sub> C- <i>p</i> -tolyl)( <i>p</i> -tolyl)(CO) <sub>2</sub> (PPh <sub>3</sub> ) <sub>2</sub> (6c)	2023 1950	1716s, 1373m, 1272s, 1222s, 1202s, 1188s, (CH <sub>2</sub> OC[O]R) 1009w, 934s, 858m, 799s, ( <i>p</i> -tolyl)
[Ru(=C(Ph)OCH <sub>2</sub> )(CO) <sub>2</sub> (PPh <sub>3</sub> ) <sub>2</sub> ] <sub>2</sub> ClO <sub>4</sub> (7a)	2054 1994	1348m, 1309m, 1256m, 944s, ( $\eta^2\text{-C(Ph)OCH}_2$ )
[Ru(=C( <i>o</i> -tolyl)OCH <sub>2</sub> )- (CO) <sub>2</sub> (PPh <sub>3</sub> ) <sub>2</sub> ] <sub>2</sub> ClO <sub>4</sub> (7b)	2059 1992	1602w, 1346m, 1309w, 1241m, 940s, 851w, ( $\eta^2\text{-C(R)OCH}_2$ )
[Os(=C( <i>o</i> -tolyl)OCH <sub>2</sub> )(CO) <sub>2</sub> - (PPh <sub>3</sub> ) <sub>2</sub> ] <sub>2</sub> ClO <sub>4</sub> (7d)	2048 1989	1601w, 1353m, 1312m, 1250s, 946s, 852w, ( $\eta^2\text{-C(R)OCH}_2$ )
[Ru(=C(Ph)OCH <sub>2</sub> )(CN- <i>p</i> -tolyl) <sub>2</sub> - (PPh <sub>3</sub> ) <sub>2</sub> ] <sub>2</sub> ClO <sub>4</sub> (8a)		2126s, 2088s, 2033w, $\nu(\text{C-N})$ 1501m, (CNR) 1337m, 1305m, 1252m, 942s, ( $\eta^2\text{-C(Ph)OCH}_2$ ) 815s, ( <i>p</i> -tolyl)
OsCl(=C( <i>o</i> -tolyl)OCH <sub>2</sub> )(CO)(PPh <sub>3</sub> ) <sub>2</sub> (9)	1921s,	1599m, 1566w, 1322m, 1236s, 1122m, 953m, 842w, ( $\eta^2\text{-C(R)OCH}_2$ ) 256m, $\nu(\text{Os-Cl})$

<sup>a</sup> In cm<sup>-1</sup>. Spectra recorded as a nujol mull between KBr or CsI plates and calibrated with polystyrene. Bands due to triphenylphosphine ligands not included. <sup>b</sup> All carbonyl bands are strong unless indicated otherwise, s, strong; m, medium; w, weak; sh, shoulder; cs, crystal splitting band.

The two metallaoxetene complexes **7d** and **9** have almost identical bands in the IR spectra which can be attributed to the metallaoxetene ring at 1322m, 1236s, and 1953m cm<sup>-1</sup> (Table 13). There is, however, an Os-Cl stretching band at 256 cm<sup>-1</sup> in **9** that is absent in **7d**. The NMR characteristics of these two molecules (Table 14) are also very similar.

(Continued on p. 440)

Table 14.  $^1\text{H}$  and  $^{13}\text{C}$  NMR spectroscopic data <sup>a</sup> for new compounds

Compound	$^1\text{H}$ NMR data	$^{13}\text{C}$ NMR data
RuCl( $\eta^2$ -C[O]Ph)(=CH <sub>2</sub> )- (PPh <sub>3</sub> ) <sub>2</sub> (2a)	15.73(t, <sup>3</sup> J(HP) 13.8,2,CH <sub>2</sub> )	
RuCl( $\eta^2$ -C[O]- <i>o</i> -tolyl)- (=CH <sub>2</sub> )(PPh <sub>3</sub> ) <sub>2</sub> (2b)	15.60(t, <sup>3</sup> J(HP) 13.9,2,CH <sub>2</sub> ); 6.98(t, <sup>3</sup> J(HH) 7.5,1,C <sub>6</sub> H <sub>4</sub> ); 6.65(d, <sup>3</sup> J(HH) 7.5,1,C <sub>6</sub> H <sub>4</sub> ); 6.53(d, <sup>3</sup> J(HH) 7.5,1,C <sub>6</sub> H <sub>4</sub> ); 6.01(d, <sup>3</sup> J(HH) 7.8,1,C <sub>6</sub> H <sub>4</sub> ); 1.91(s,3,CH <sub>3</sub> )	292.5(s,C[O]R); 262.3(t, <sup>2</sup> J(CP) 8.6,CH <sub>2</sub> ); 138.4,135.8,131.4,130.84,124.89 (s,C <sub>6</sub> H <sub>4</sub> ); 135.0(t, <sup>2</sup> J(CP) 5.4,PPh <sub>3</sub> C( <i>ortho</i> )); 132.4(t, <sup>1</sup> J(CP) 20.4,PPh <sub>3</sub> C( <i>ipso</i> )); 130.07(s,PPh <sub>3</sub> C( <i>para</i> )); 128.35(t, <sup>3</sup> J(CP) 4.6,PPh <sub>3</sub> C( <i>meta</i> ))
RuCl( $\eta^2$ -C[O]- <i>p</i> -tolyl)- (=CH <sub>2</sub> )(PPh <sub>3</sub> ) <sub>2</sub> (2c)	15.74(t, <sup>3</sup> J(HP) 13.8,2,CH <sub>2</sub> ); 7.44(d, <sup>3</sup> J(HH) 7.7,2,C <sub>6</sub> H <sub>4</sub> ); 6.65(d, <sup>3</sup> J(HH) 8.1,2,C <sub>6</sub> H <sub>4</sub> ); 2.25(s,3,CH <sub>3</sub> )	279.47(t, <sup>2</sup> J(CP) 13.1,C[O]R); 261.2(t, <sup>2</sup> J(CP) 8.6,2,CH <sub>2</sub> ); 142.47,138.37,129.11,127.61(s,C <sub>6</sub> H <sub>4</sub> ); 134.68(t, <sup>2</sup> J(CP) 5.6,PPh <sub>3</sub> C( <i>ortho</i> )); 132.27(t, <sup>1</sup> J(CP) 20.5,PPh <sub>3</sub> C( <i>ipso</i> )); 130.07(s,PPh <sub>3</sub> C( <i>para</i> )); 128.32(t, <sup>3</sup> J(CP) 4.7,PPh <sub>3</sub> C( <i>meta</i> ))
OsCl( $\eta^2$ -C[O]- <i>o</i> -tolyl)- (=CH <sub>2</sub> )(PPh <sub>3</sub> ) <sub>2</sub> (2d)	16.94(t, <sup>3</sup> J(HP) 13.6,2,CH <sub>2</sub> ); 7.05(td, <i>J</i> (HH) 7.4, <i>J</i> (HH) 1.32,1,C <sub>6</sub> H <sub>4</sub> ); 6.67(dbr, <i>J</i> (HH) 7.3,1,C <sub>6</sub> H <sub>4</sub> ); 6.61(tbr, <i>J</i> (HH) 7.4,1,C <sub>6</sub> H <sub>4</sub> ); 6.33(dd, <i>J</i> (HH) 7.8,1.1,1,C <sub>6</sub> H <sub>4</sub> ); 1.85(s,3,CH <sub>3</sub> )	249.26(t, <sup>2</sup> J(CP) 5.8,CH <sub>2</sub> ); 138.78,136.10,135.50,129.52, 128.71,124.99(s,C <sub>6</sub> H <sub>4</sub> ); 135.15(t, <sup>2</sup> J(CP) 5.2,PPh <sub>3</sub> C( <i>ortho</i> )); 132.45(t, <sup>1</sup> J(CP) 23.8,PPh <sub>3</sub> C( <i>ipso</i> )); 130.09(s,PPh <sub>3</sub> C( <i>para</i> )); 128.30(t, <sup>3</sup> J(CP) 4.9,PPh <sub>3</sub> C( <i>meta</i> )); 22.37(s,CH <sub>3</sub> )
RuBr( $\eta^2$ -C[O]Ph)(=CH <sub>2</sub> )- (PPh <sub>3</sub> ) <sub>2</sub> (3a)	15.78(t, <sup>3</sup> J(HP) 14,2,CH <sub>2</sub> )	
RuI( $\eta^2$ -C[O]Ph)(=CH <sub>2</sub> )- (PPh <sub>3</sub> ) <sub>2</sub> (4a)	15.73(t, <sup>3</sup> J(HP) 14,2,CH <sub>2</sub> )	
Ru(CH <sub>2</sub> OC[O]Me)(Ph) (CO)(PPh <sub>3</sub> ) <sub>2</sub> (5a)	6.45(sbr,5,C <sub>6</sub> H <sub>5</sub> ); 5.40(t, <sup>3</sup> J(HP) 9.1,2,CH <sub>2</sub> ); 0.66(s,3,CH <sub>3</sub> )	210.84(t, <sup>2</sup> J(CP) 17.8,3,CO); 181.50(s,CH <sub>3</sub> CO <sub>2</sub> ); 166.31(t, <sup>2</sup> J(CP) 11.0, Ph C( <i>ipso</i> )); 141.37,125.19,119.70(s,C <sub>6</sub> H <sub>5</sub> ); 134.46(t, <sup>2</sup> J(CP) 5.3,PPh <sub>3</sub> C( <i>ortho</i> )); 133.45(t, <sup>1</sup> J(CP) 20.3,PPh <sub>3</sub> C( <i>ipso</i> )); 129.39(s,PPh <sub>3</sub> C( <i>para</i> )); 128.03(t, <sup>3</sup> J(CP) 4.5,PPh <sub>3</sub> C( <i>meta</i> ))
Ru(CH <sub>2</sub> OC[O]Me)- ( <i>p</i> -tolyl)(CO)(PPh <sub>3</sub> ) <sub>2</sub> (5c)	5.34(t, <sup>3</sup> J(HP) 4.5,2,CH <sub>2</sub> ); 2.02(s,3,C <sub>6</sub> H <sub>4</sub> CH <sub>3</sub> ); 0.70(s,3,CH <sub>3</sub> CO <sub>2</sub> )	
Os(CH <sub>2</sub> OC[O]CH <sub>3</sub> )- ( <i>o</i> -tolyl)(CO)(PPh <sub>3</sub> ) <sub>2</sub> (5d)	4.94(sbr,2,CH <sub>2</sub> ); 2.20(s,3,C <sub>6</sub> H <sub>4</sub> CH <sub>3</sub> ); 0.31(s,3,CH <sub>3</sub> CO <sub>2</sub> )	
Ru(CH <sub>2</sub> OC[O]- <i>p</i> -tolyl)(Ph)- (CO)(PPh <sub>3</sub> ) <sub>2</sub> (5e)	5.58(t, <sup>3</sup> J(HP) 9,2,CH <sub>2</sub> ); 2.30(s,3,C <sub>6</sub> H <sub>4</sub> CH <sub>3</sub> )	
Ru(CH <sub>2</sub> OC[O]- <i>p</i> -tolyl)- ( <i>p</i> -tolyl)(CO)(PPh <sub>3</sub> ) <sub>2</sub> (5f)	7.22(d, <sup>3</sup> J(HH) 7.6,2,C <sub>6</sub> H <sub>4</sub> CH <sub>3</sub> ); 6.97(d, <sup>3</sup> J(HH) 8.1,2,C <sub>6</sub> H <sub>4</sub> CH <sub>3</sub> ); 6.90(d, <sup>3</sup> J(HH) 8.1,2,C <sub>6</sub> H <sub>4</sub> CH <sub>3</sub> ); 6.38(d, <sup>3</sup> J(HH) 7.6,2,C <sub>6</sub> H <sub>4</sub> CH <sub>3</sub> ); 5.53(t, <sup>3</sup> J(HP) 9.1,2,CH <sub>2</sub> );	

Table 14 (continued)

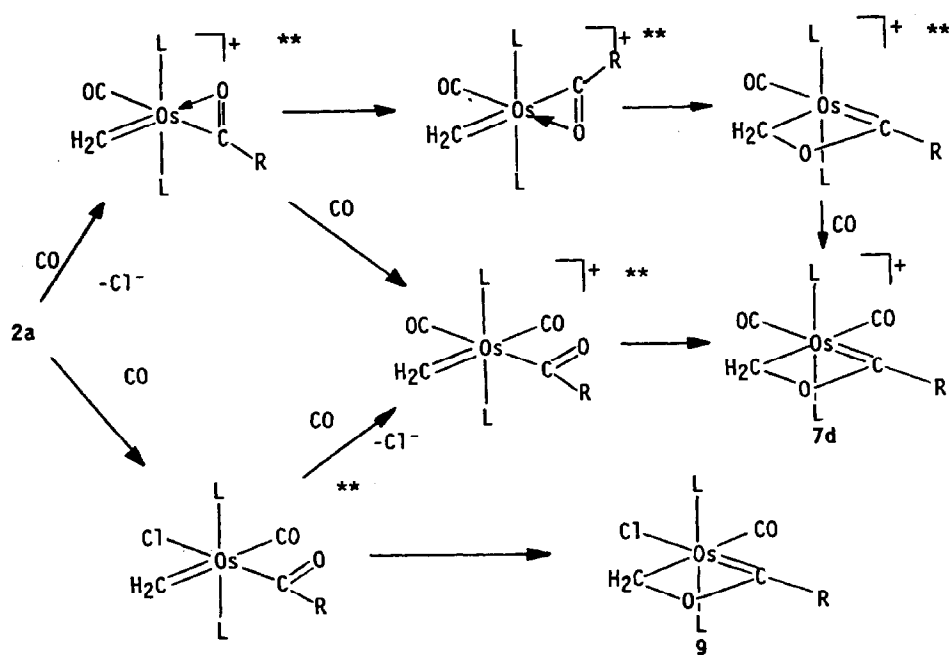
Compound	<sup>1</sup> H NMR data	<sup>13</sup> C NMR data
Ru(CH <sub>2</sub> O <sub>2</sub> CCH <sub>3</sub> )(Ph)- (CO) <sub>2</sub> (PPh <sub>3</sub> ) <sub>2</sub> (6a)	2.33(s,3,C <sub>6</sub> H <sub>4</sub> CH <sub>3</sub> ); 2.07(s,3,C <sub>6</sub> H <sub>4</sub> CH <sub>3</sub> ) 6.82(sbr,2,C <sub>6</sub> H <sub>5</sub> ); 6.59(dbr, J(HH) 2.7,3C <sub>6</sub> H <sub>5</sub> ); 3.95(t, <sup>3</sup> J(HP) 9.5,2,CH <sub>2</sub> )	200.15(t, <sup>2</sup> J(CP) 10.2, C O); 199.9(t, <sup>3</sup> J(CP) 10.5, C O); 154.95(t, <sup>2</sup> J(CP) 13.3, Ph C( <i>ipso</i> )); 143.33,127.12,122.99(s, C <sub>6</sub> H <sub>5</sub> ); 134.57(t, <sup>2</sup> J(CP) 5.1, PPh <sub>3</sub> C( <i>ortho</i> )); 133.36(t, <sup>1</sup> J(CP) 21.8, PPh <sub>3</sub> C( <i>ipso</i> )); 130.18(s, PPh <sub>3</sub> C( <i>para</i> )); 128.13(t, <sup>3</sup> J(CP) 4.6, PPh <sub>3</sub> C( <i>metal</i> ))
Ru(CH <sub>2</sub> O <sub>2</sub> C- <i>p</i> -tolyl)- ( <i>p</i> -tolyl)(CO) <sub>2</sub> (PPh <sub>3</sub> ) <sub>2</sub> (62)	4.00(t, <sup>3</sup> J(HP) 10,2,CH <sub>2</sub> ); 2.11(s,3,C <sub>6</sub> H <sub>4</sub> CH <sub>3</sub> ); 1.81(s,3,CH <sub>3</sub> CO <sub>2</sub> )	
[Ru(=C(Ph)OCH <sub>2</sub> )(CO) <sub>2</sub> - (PPh <sub>3</sub> ) <sub>2</sub> ]ClO <sub>4</sub> (7a)	4.78(t, <sup>3</sup> J(HP) 3.5,2,CH <sub>2</sub> )	
[Ru(=C( <i>o</i> -tolyl)OCH <sub>2</sub> )- (CO) <sub>2</sub> (PPh <sub>3</sub> ) <sub>2</sub> ]ClO <sub>4</sub> (7b)	4.76(t, <sup>3</sup> J(HP) 3,2,CH <sub>2</sub> );  1.44(s,2,CH <sub>3</sub> )	
[Os(=C( <i>o</i> -tolyl)OCH <sub>2</sub> )- (CO) <sub>2</sub> (PPh <sub>3</sub> ) <sub>2</sub> ]ClO <sub>4</sub> (7d)	7.14(tbr, J(HH) 7.6,1,C <sub>6</sub> H <sub>4</sub> ); 7.01(tbr, J(HH) 7.4,1,C <sub>6</sub> H <sub>4</sub> ); 6.94(d, J(HH) 7.5,1,C <sub>6</sub> H <sub>4</sub> ); 6.85(tbr, J(HH) 7.2,1,C <sub>6</sub> H <sub>4</sub> ); 4.81(t, <sup>3</sup> J(HP) 4.4,2,CH <sub>2</sub> ); 1.41(s,3,CH <sub>3</sub> )	216.01(t, <sup>2</sup> J(CP) 7.0,=C(Ph)O); 182.36(t, <sup>2</sup> J(CP) 10.4, C O); 181.71(t, <sup>2</sup> J(CP) 6.1, C O); 140.83,140,137.75,137.63, 136.77,121.93(s, C <sub>6</sub> H <sub>4</sub> CH <sub>3</sub> ); 133.68(t, <sup>2</sup> J(CP) 5.5, PPh <sub>3</sub> C( <i>ortho</i> )); 132.34(s, PPh <sub>3</sub> C( <i>para</i> )); 129.98(t, <sup>1</sup> J(CP) 28.1, PPh <sub>3</sub> C( <i>ipso</i> )); 129.61(t, <sup>3</sup> J(CP) 5.3, PPh <sub>3</sub> C( <i>meta</i> )); 45.05(t, <sup>2</sup> J(CP) 7.7, CH <sub>2</sub> ); 23.93(s,3,CH <sub>3</sub> )
[Ru(=C(Ph)OCH <sub>2</sub> )(CN- <i>p</i> - tolyl) <sub>2</sub> (PPh <sub>3</sub> ) <sub>2</sub> ]ClO <sub>4</sub> (8a)	7.41(m,2,C <sub>6</sub> H <sub>5</sub> ); 7.35(tbr, J(HH) 7.2,1,C <sub>6</sub> H <sub>5</sub> ); 7.26(m,2,C <sub>6</sub> H <sub>5</sub> ); 7.08(d, <sup>3</sup> J(HH) 8.2,2,C <sub>6</sub> H <sub>4</sub> CH <sub>3</sub> ); 6.96(d, <sup>3</sup> J(HH) 8.1,2,C <sub>6</sub> H <sub>4</sub> CH <sub>3</sub> ); 6.41(d, <sup>3</sup> J(HH) 8.2,2,C <sub>6</sub> H <sub>4</sub> CH <sub>3</sub> ); 6.21(d, <sup>3</sup> J(HH) 8.2,2,C <sub>6</sub> H <sub>4</sub> CH <sub>3</sub> ); 4.77(t, <sup>3</sup> J(HP) 3.1,2,CH <sub>2</sub> ); 2.34(s,3,C <sub>6</sub> H <sub>4</sub> CH <sub>3</sub> ); 2.27(s,3,C <sub>6</sub> H <sub>4</sub> CH <sub>3</sub> )	296.80(t, <sup>2</sup> J(CP) 8.3,=C(Ph)O); 163.70(t, <sup>2</sup> J(CP) 10.7, C NR); 161.60(t, <sup>2</sup> J(CP) 17.5, C NR); Aromatic singlets at: 140.70,140.35, 139.86,135.67,130.61,130.54,128.57, 125.97,125.27,124.94; 133.83(t, <sup>2</sup> J(CP) 5.5, PPh <sub>3</sub> C( <i>ortho</i> )); 132.98(t, <sup>1</sup> J(CP) 22.7, PPh <sub>3</sub> C( <i>ipso</i> )); 131.03(s, PPh <sub>3</sub> C( <i>para</i> )); 128.97(t, <sup>3</sup> J(CP) 4.6, PPh <sub>3</sub> C( <i>metal</i> )); 64.02(t, <sup>2</sup> J(CP) 9.7, CH <sub>2</sub> ); 21.72(s, CH <sub>3</sub> )
[OsCl(=C( <i>o</i> -tolyl)OCH <sub>2</sub> )- (CO)(PPh <sub>3</sub> ) <sub>2</sub> ] (9)	7.44(dd, <sup>3</sup> J(HH) 7.9,1.2,1,C <sub>6</sub> H <sub>4</sub> ); 7.07(td, <sup>3</sup> J(HH) 7.5,1.3,1,C <sub>6</sub> H <sub>4</sub> ); 6.69(td, <sup>3</sup> J(HH) 7.9,1,1,C <sub>6</sub> H <sub>4</sub> );  6.55(dbr, <sup>3</sup> J(HH) 7.5,1,1,C <sub>6</sub> H <sub>4</sub> ); 4.96(t, <sup>3</sup> J(HP) 5.1,2,CH <sub>2</sub> ); 1.42(s,3,CH <sub>3</sub> )	257.29(t, <sup>2</sup> J(CP) 6.0,=C(R)O); 189.62(t, <sup>2</sup> J(CP) 8.5, C O); 137.65,136.94,131.85,131.81,125.71 (s, C <sub>6</sub> H <sub>4</sub> ); 134.80(t, <sup>2</sup> J(CP) 5.3, PPh <sub>3</sub> C( <i>ortho</i> )); 133.48(t, <sup>1</sup> J(CP) 25.6, PPh <sub>3</sub> C( <i>ipso</i> )); 130.14(s, PPh <sub>3</sub> C( <i>para</i> )); 128.20(t, <sup>3</sup> J(CP) 4.9, PPh <sub>3</sub> C( <i>metal</i> )); 55.14(t, <sup>2</sup> J(CP) 8.8, CH <sub>2</sub> ); 23.70(s, CH <sub>3</sub> )

<sup>a</sup> As chloroform solutions at 21 °C. Chemical shifts are in ppm with respect to tetramethylsilane and coupling constants are given in Hertz.

In an attempt to elucidate the factors which control the formation of this pair of complexes from the carbonylation of **2d** the following experiments have been performed:

- (1) A purified sample (see Experimental) of **9** was carbonylated using the same conditions that were used in the carbonylation of **2d**. Only starting material was recovered and there was no evidence for the formation of the dicarbonyl complex **7d** during this reaction.
- (2) Lithium chloride (200 mg), dissolved in 2 ml methanol, was added to a dichloromethane solution of **2d**. Carbonylation of this mixture with the aforementioned conditions resulted in the same product distribution, as estimated by the relative intensities of the  $\nu(\text{CO})$  bands in the IR spectrum.
- (3) The influence of the solvent on the product distribution was assessed by conducting the reaction in a polar solvent mixture (1/50 dichloromethane/methanol) and in an apolar solvent pair (1/50 dichloromethane/carbon tetrachloride). The product distribution in each case was identical (again, as estimated by the intensity of the  $\nu(\text{CO})$  bands in the IR spectrum).

The most significant result of the above experiments is that **7d** is not formed during the carbonylation of **9**. Heating a dichloromethane solution of **7d** with [PPN]I at reflux for 1 h, was carried out to ascertain the lability of the carbon monoxide. Starting material was recovered from this reaction and there was no indication that a neutral iodo complex analogous to **9** was formed. In a separate



\*\* = proposed intermediates

experiment, the ruthenium complex **7a** was treated with [PPN]I in this manner, with the same result. The dicarbonyl complex **7d** and the monocarbonyl complex **9** do not interconvert and it is likely that they are formed by different mechanisms. A possible set of reactions which would account for these observations is set out above. In all but one case the last proposed step is the combination of the acyl and methylene ligands to give **7d** or **9**. There is no tendency for the methylene complexes to undergo this reaction in the absence of carbon monoxide or isocyanide and the attack of the oxygen on the methylene suggests an increase in the electrophilicity at the carbon. The most sensible origin of this increase is either the generation of a cationic complex, through loss of chloride, or introduction of  $\pi$ -acid ligands such as carbon monoxide or isocyanide. These ligands would effectively remove  $\pi$ -electron density from the methylene, and thus render it more susceptible to nucleophilic attack.

When **2a** is treated with one equivalent of *p*-tolylisocyanide a mixture of starting material and the bis(*p*-tolylisocyanide) complex analogous to **8a** are obtained. This result suggests that the rate of uptake of the second isocyanide is more rapid than the initial substitution although it does not indicate the mechanism by which the first isocyanide is incorporated.

Proposed mechanisms for the Fischer-Tropsch reaction often invoke migratory insertion of the growing alkyl chain onto terminal methylene or other alkyldiene ligands. Research aimed at finding soluble catalysts for CO reduction often assume that a similar sequence of reactions will operate at a single metal centre. However, the reactions described in this paper indicate that in the development of any homogeneous catalyst for CO/H<sub>2</sub> reactions based on mononuclear systems, account will have to be taken of other competing reactions of the methylene ligand, particularly metallaoxetene formation.

## Conclusion

The chemistry of  $\text{MCl}(\text{NO})(=\text{CH}_2)(\text{PPh}_3)_2$  [2,45] and  $\text{MCl}(\eta^2\text{-C[O]R})(=\text{CH}_2)(\text{PPh}_3)_2$  make for an interesting contrast. The difference in the reactivity patterns associated with these two methylene complexes reflects the fundamental difference in the reactions of divalent and zerovalent ruthenium and osmium. In the case of the  $d^8$  nitrosyl methylene complex, electrophiles such as HX, X<sub>2</sub>, HgX<sub>2</sub>, SO<sub>2</sub> and AuI readily add across the metal-carbon bond. While it is tempting to describe the reactivity of the carbene ligand in these complexes as nucleophilic, the site of initial electrophilic attack remains uncertain.

On the other hand, the divalent methylene complexes **2** do not react with electrophiles, nor with nucleophiles that usually add to electrophilic methylene complexes, i.e. pyridine or triphenylphosphine. However, incipient nucleophiles (within the coordination sphere of the metal) such as the oxygen atoms of the coordinated  $\eta^2$ -acyl and the uncoordinated oxygen of a carboxylato ligand do add to the methylene ligand. Unexpectedly, the coordinated aryl migrates onto the CO ligand rather than methylene. A suitable explanation for this must await a further detailed study.

## Experimental

The general techniques and instrumentation used in this work have been described before [46,47]. Except when specifically mentioned below, the following preparations and reactions were conducted in dried solvents in the open.

### *RuCl(Ph)(CO)(PPh<sub>3</sub>)<sub>2</sub> (1a)*

RuHCl(CO)(PPh<sub>3</sub>)<sub>3</sub>, 1.00 g, and HgPh<sub>2</sub>, 0.44 g, were heated under reflux in toluene, 50 ml, for 15 min. The resulting deep red solution was cooled and the elemental mercury was removed by filtration through a celite pad. Ethanol, 100 ml, was added and the solvent volume was reduced in vacuo to afford **1a**, 0.79 g (98%), as deep red prisms m.p. 214–216°C. Anal. Found: C, 67.12; H, 4.78. C<sub>43</sub>H<sub>35</sub>ClOP<sub>2</sub>Ru calcd.: C, 67.41; H, 4.60%.

### *RuCl(o-tolyl)(CO)(PPh<sub>3</sub>)<sub>2</sub> (1b)*

RuHCl(CO)(PPh<sub>3</sub>)<sub>3</sub>, 2.0 g, and of Hg(*o*-tolyl)<sub>2</sub>, 1.0 g, were heated under reflux in benzene, 20 ml, for 18 h. The resulting dark orange solution was cooled and filtered through a celite pad to remove the elemental mercury. Ethanol, 30 ml, was added and the solvent volume was reduced in vacuo to afford **1b**, 1.53 g (93%) as orange needles m.p. 210–213°C. Anal. Found: C, 67.66; H, 4.74. C<sub>44</sub>H<sub>37</sub>ClOP<sub>2</sub>Ru calcd.: C, 67.73; H, 4.78%.

### *RuCl(p-tolyl)(CO)(PPh<sub>3</sub>)<sub>2</sub> (1c)*

RuHCl(CO)(PPh<sub>3</sub>)<sub>3</sub>, 2.00 g, and Hg(*p*-tolyl)<sub>2</sub>, 0.95 g, were heated under reflux in toluene, 50 ml, for 15 min. The deep red solution was allowed to cool to room temperature and the resulting red crystals were removed by filtration. This product was then dissolved in dichloromethane and filtered through a celite pad to remove the elemental mercury. Ethanol, 50 ml, was added and the solvent volume was reduced in vacuo to afford **1c**, 1.55 g (94%), as red crystals, m.p. 204–206°C. Anal. Found: C, 67.77; H, 4.75. C<sub>44</sub>H<sub>37</sub>ClOP<sub>2</sub>Ru calcd.: C, 67.73; H, 4.78%.

### *OsCl(o-tolyl)(CO)(PPh<sub>3</sub>)<sub>2</sub> (1d)*

OsHCl(CO)(PPh<sub>3</sub>)<sub>3</sub>, 2 g, and Hg(*o*-tolyl)<sub>2</sub>, 1.15 g, were heated under reflux in toluene, 150 ml, for 20 min. The resulting red solution was cooled, filtered through a celite pad, and, after the addition of ethanol, 200 ml, the solvent volume was reduced in vacuo to afford **1d**, 1.5 g (90%), as red microcrystals, m.p. 190–195°C. Anal. Found: C, 60.49; H, 4.51. C<sub>44</sub>H<sub>37</sub>ClOOSp<sub>2</sub> calcd.: C, 60.79; H, 4.29%.

### *RuCl(η<sup>2</sup>-C[O]Ph)(=CH<sub>2</sub>)(PPh<sub>3</sub>)<sub>2</sub> (2a)*

RuCl(Ph)(CO)(PPh<sub>3</sub>)<sub>2</sub>, 0.1 g, was dissolved in dichloromethane, 20 ml, and an ether solution of diazomethane [48] (~ 5 M, 30 ml) was added dropwise over 20 min during which the solution became a deep black and there was slow, but steady, evolution of dinitrogen. Occasionally there was a precipitate of product towards the end of the addition. Ethanol, 50 ml, was then added to the reaction mixture and a dark black-orange product was recovered by concentrating this mixture in vacuo. This product was purified by column chromatography on silica gel (3 × 15 cm) using dichloromethane, 100 ml, as eluant. In some cases, usually when there was considerable decomposition, this chromatography step was repeated. Final recryst-



tallization from dichloromethane/ethanol returned bright yellow-orange plates of **2a**, 0.053 g, 52%, m.p. 163°C. Anal. (as 1/2 dichloromethane solvate as confirmed by <sup>1</sup>H NMR) Found: C, 65.07; H, 5.05. C<sub>44</sub>H<sub>37</sub>ClOP<sub>2</sub>Ru · ½CH<sub>2</sub>Cl<sub>2</sub> calcd.: C, 64.97; H, 4.66%.

*RuCl(η<sup>2</sup>-C[O]-*o*-tolyl)(=CH<sub>2</sub>)(PPh<sub>3</sub>)<sub>2</sub> (2b)*

RuCl(*o*-tolyl)(CO)(PPh<sub>3</sub>)<sub>2</sub>, 0.53 g, in dichloromethane, 10 ml, was treated as for **2a**. After chromatography on silica gel the product was recrystallized from dichloromethane/ethanol to give **2b**, 0.24 g, 45%, m.p. 161°C (plates). Anal. (as ½ dichloromethane solvate as confirmed by <sup>1</sup>H NMR) Found: C, 65.98; H, 4.82. C<sub>45</sub>H<sub>39</sub>ClOP<sub>2</sub>Ru · ½CH<sub>2</sub>Cl<sub>2</sub> calcd.: C, 66.19; H, 4.87%.

*RuCl(η<sup>2</sup>-C[O]-*p*-tolyl)(=CH<sub>2</sub>)(PPh<sub>3</sub>)<sub>2</sub> (2c)*

RuCl(*p*-tolyl)(CO)(PPh<sub>3</sub>)<sub>2</sub>, 2.5 g, was suspended in dichloromethane, 100 ml, and an ether solution of diazomethane (≈ 5 M, 50 ml) was added dropwise over the course of 20 min. During this period the red suspension gradually dissolved and a black solution formed. Diazomethane addition was continued until all of the red starting material had dissolved and gas evolution had subsided. Ethanol, 100 ml, was then added and this mixture was allowed to stand for a further 15 min and then the dichloromethane was removed in vacuo. The resulting solid purified by column chromatography on silica gel (10 × 15 cm) and 250 ml dichloromethane was used as an eluant. An equal volume of ethanol was then added to the eluted solution and the product recrystallized by removing the dichloromethane in vacuo. This returned **2c**, 1.8 g, 71%, m.p. 149°C (dec) as yellow flakes. Anal. Found: C, 68.00; H, 5.09. C<sub>45</sub>H<sub>39</sub>ClOP<sub>2</sub>Ru calcd.: C, 68.04; H, 4.96%.

*OsCl(η<sup>2</sup>-C[O]-*o*-tolyl)(=CH<sub>2</sub>)(PPh<sub>3</sub>)<sub>2</sub> (2d)*

OsCl(*o*-tolyl)(CO)(PPh<sub>3</sub>)<sub>2</sub>, 1.0 g, was dissolved in dichloromethane, 50 ml, and was treated with an ether solution of diazomethane (≈ 5 M, 50 ml) which was added dropwise. The bright burgundy colour of the starting material faded rapidly and as the addition of diazomethane proceeded the reaction mixture darkened rapidly and, occasionally, the product formed a yellow precipitate towards the end of the addition. This material was treated as for **2c** and the product was purified by column chromatography on silica gel (3 × 10 cm) and with dichloromethane, 200 ml, used as an eluant. To the eluate ethanol, 100 ml, was added and the product was recovered by reduction of the solvent volume in vacuo to give **2d**, 0.73 g, 72%, m.p. 180°C (yellow prisms). Anal. (as ½ dichloromethane solvate as confirmed by <sup>1</sup>H NMR) Found: C, 59.60; H, 4.72. C<sub>45</sub>H<sub>39</sub>ClOOSp<sub>2</sub> · ½CH<sub>2</sub>Cl<sub>2</sub> calcd.: C, 59.72; H, 4.39%. Crystals suitable for X-ray diffraction were grown from dichloromethane/ether under nitrogen at -20°C.

*RuX(η<sup>2</sup>-C[O]Ph)(=CH<sub>2</sub>)(PPh<sub>3</sub>)<sub>2</sub> (3a: X = Br; 4a, X = I)*

RuCl(η<sup>2</sup>-C[O]Ph)(=CH<sub>2</sub>)(PPh<sub>3</sub>)<sub>2</sub> (**2a**) 0.1 g, was dissolved in dichloromethane, 10 ml, and a solution of either lithium bromide or lithium iodide, 0.25 g, previously dissolved in a minimum of water, ca. 2 ml, and diluted with ethanol, 25 ml, was then added. This solution was immediately recrystallized by removing the dichloromethane in vacuo to give a yellow-orange (**3a**) or gold (**4a**) solid. The above procedure was repeated again to ensure complete metathesis, although more dichlo-

romethane was required to dissolve the less soluble bromide and iodide derivatives.

**3a:** Isolated as yellow-orange plates, 0.083 g, 79%, m.p. 159–161°C. Anal. Found: C, 63.98; H, 4.96.  $C_{44}H_{37}BrOP_2Ru$  calcd.: C, 64.08; H, 4.53%.

**4a:** Isolated as gold coloured plates, 0.11 g, 98% yield, m.p. 156–157°C. Anal. Found: C, 60.80; H, 4.78.  $C_{44}H_{37}IOP_2Ru$  calcd.: C, 60.62; H, 4.29%.

$\overline{Ru(CH_2OC[O]R)(Ph)(CO)(PPh_3)_2}$  (**5a**:  $R = Me$ ; **5e**:  $R = p\text{-tolyl}$ )

$RuCl(\eta^2-C[O]Ph)(=CH_2)(PPh_3)_2$  (**2a**) 0.1 g, was dissolved in dichloromethane, 10 ml, and then treated with a solution of either sodium acetate, 0.2 g, (for **5a**) or sodium 4-methylbenzoate, 0.25 g, (for **5e**), prepared by dissolving the salt in a minimum of water and then diluting this solution with ethanol, 50 ml. In each case these reaction mixtures were stirred for 45 min and then the product was crystallized by concentrating the solvent in vacuo.

**5a:** Light yellow plates of the product were filtered and washed thoroughly with water, methanol, ethanol and finally n-hexane. This product was sufficiently pure for most purposes but for microanalysis it was recrystallized from dichloromethane/ethanol. Yield, 0.08 g, 78%, m.p. 164–166°C. Anal. (as  $\frac{1}{4}$  dichloromethane solvate as confirmed by  $^1H$  NMR) Found: C, 68.08; H, 5.22.  $C_{46}H_{40}O_3P_2Ru \cdot \frac{1}{4}CH_2Cl_2$  calcd.: C, 68.01; H, 4.99%. Crystals suitable for X-ray diffraction were grown from dichloromethane/ethanol.

**5e:** Isolated as cream needles after purification as above. Yield, 0.08 g, 71%, 0.08 g, m.p. 145°C. Anal. Found: C, 70.23; H, 5.50.  $C_{52}H_{44}O_3P_2Ru$  calcd.: C, 70.97; H, 5.05%.

$\overline{Ru(CH_2OC[O]R)(p\text{-tolyl})(CO)(PPh_3)_2}$  (**5c**:  $R = Me$ ; **5f**:  $R = p\text{-tolyl}$ )

$RuCl(\eta^2-C[O]p\text{-tolyl})(=CH_2)(PPh_3)_2$  (**2c**), was treated with either sodium acetate or sodium 4-methylbenzoate as described above for **5a** and **5e**.

**5c:** A dichloromethane solution, 10 ml, of **2c**, 0.2 g, was treated with sodium acetate, 0.5 g, dissolved in water/ethanol. The orange-yellow colour of **2c** faded rapidly and was replaced by a light yellow coloured solution. After 15 min the dichloromethane was removed in vacuo and **5c** was recovered as a light yellow solid, 0.17 g, 82%, after, filtration and washing thoroughly with water, methanol and ethanol. This product was spectroscopically characterized and the data for this complex is included in Tables 13 and 14.

**5f:** As above, **2c**, 0.12 g, was treated with sodium 4-methylbenzoate, 0.5 g, for 50 min. The product was recrystallized twice from dichloromethane/ethanol to give **5f**, 0.08 g, 59% as pale yellow needles, m.p. 165–167°C. Anal. (as  $\frac{1}{3}$  dichloromethane solvate as confirmed by  $^1H$  NMR) Found: C, 70.25; H, 5.66.  $C_{53}H_{46}O_3P_2Ru \cdot \frac{1}{3}CH_2Cl_2$  calcd.: C, 70.14; H, 5.14%.

$\overline{Os(CH_2OC[O]CH_3)(o\text{-tolyl})(CO)(PPh_3)_2}$  (**5d**)

$OsCl(\eta^2-C[O]o\text{-tolyl})(=CH_2)(PPh_3)_2$  (**2d**) 0.07 g, in dichloromethane, 10 ml, was treated with sodium acetate, 0.24 g, in ethanol/water. This mixture was stirred for 2 h at room temperature and the colourless needles of **5d**, 0.055 g, 77%, m.p. 160°C, were recovered by removing the dichloromethane in vacuo. Subsequent recrystallization resulted in a very poor return ( $\approx 20\%$ ) of **5d**. Anal. (as  $\frac{1}{2}$  dichloromethane solvate as confirmed by  $^1H$  NMR) Found: C, 60.73; H, 4.57.  $C_{47}H_{42}O_3OsP_2 \cdot \frac{1}{2}CH_2Cl_2$  calcd.: C, 60.08; H, 4.57%.

$Ru(CH_2O_2CCH_3)(Ph)(CO)_2(PPh_3)_2$  (**6a**)

$Ru(CH_2OC[O]CH_3)(CO)(Ph)(PPh_3)_2$  (**5a**) 0.15 g, was carbonylated in a Fischer-Porter bottle at 40 psi for 8 h at room temperature in 20 ml dichloromethane. Ethanol, 20 ml, was added to the reaction mixture afterwards and the solvent volume was reduced in vacuo to give **6a**, 0.12 g, 78%, colourless rods, m.p. 171–174° C. Anal. Found: C, 67.85; H, 4.93.  $C_{47}H_{40}O_4P_2Ru$  calcd.: C, 67.85; H, 4.86%.

$Ru(CH_2O_2C-p-tolyl)(p-tolyl)(CO)_2(PPh_3)_2$  (**6c**)

$Ru(CH_2OC[O]-p-tolyl)(p-tolyl)(CO)(PPh_3)_2$  (**5c**) 0.17 g, was treated as for **5a** above to give **6c**, 0.16 g, 91%, as fine colourless crystals. This product was spectroscopically characterized and the data for this complex are included in Tables 13 and 14.

$[Ru(=C(R)OCH_2)(CO)_2(PPh_3)_2]ClO_4$  (**7a**;  $R = Ph$ , **7b**:  $R = o-tolyl$ )

$RuCl(\eta^2-C[O]R)(=CH_2)(PPh_3)_2$ , either **2a** or **2b** were carbonylated in a Fischer-Porter bottle at 40 psi for 1 h at room temperature in dichloromethane, 20 ml. During the carbonylation the originally yellow-orange solution became a very pale yellow. Ethanol, 30 ml, and of lithium perchlorate, 0.01 g, were added to the mixture and the almost colourless products were recovered by reduction of the solvent volume in vacuo.

**7a**: Isolated as colourless needles, 0.08 g, 69% yield, from **2a**, 0.1 g, m.p. 122–123° C.

Anal. Found: C, 60.91; H, 4.97.  $C_{46}H_{37}ClO_7P_2Ru$  calcd.: C, 61.36; H, 4.15%.

**7b**: Isolated as colourless needles, 0.4 g, 72% yield, from **2b**, 0.48 g, m.p. 140° C(dec).

Anal. Found: C, 61.32; H, 5.11.  $C_{47}H_{39}ClO_7P_2Ru$  calcd.: C, 61.74; H, 4.31%.

$[Os(=C(o-tolyl)OCH_2)(CO)_2(PPh_3)_2]ClO_4$  (**7d**)

$OsCl(\eta^2-C[O]-o-tolyl)(=CH_2)(PPh_3)_2$  (**2a**) 0.105 g, was carbonylated in a Fischer-Porter bottle at 60 psi for 40 min at room temperature in dichloromethane, 20 ml. During the course of the reaction the colour of the solution changed from a orange-yellow to a light yellow. Ethanol, 40 ml, and lithium perchlorate, 0.02 g, were added and then this mixture was concentrated in vacuo until crystals just began to form, and then an equal volume of isopropanol was added. The concentration was continued until the solvent volume was about 5 ml. The light yellow solid which formed was filtered and then washed with isopropanol and n-hexane to give 0.09 g. This solid was a mixture of **7d** and **9**, the two of which were separated by column chromatography on neutral alumina as follows. The mixture is dissolved in a minimum of dichloromethane and was adsorbed onto neutral alumina, 2 g, and then placed on a column of neutral alumina (3 × 10 cm). A bright yellow band was eluted with dichloromethane, 50 ml, from which the bright yellow product **9**, 0.01 g, 10%, was obtained by crystallization using ethanol. The complex **7d** was then eluted with acetone, 200 ml. The acetone was completely removed in vacuo and the colourless residue was recrystallized from dichloromethane/ethanol to give, 0.08 g, 80% of colourless plate like needles, m.p. 184° C. Anal. Found: C, 56.31; H, 4.95.  $C_{47}H_{39}ClO_7OsP_2$  calcd.: C, 56.25; H, 3.93%.

$[Ru(=C(Ph)OCH_2)(CN-p-tolyl)_2(PPh_3)_2]ClO_4$  (**8a**)

$RuCl(\eta^2-C[O]Ph)(=CH_2)(PPh_3)_2$  (**2a**) 0.08 g, was dissolved in dichloromethane, 20 ml, and was treated with *p*-tolylisocyanide, exactly 0.028 g, 2.3 equivalents. A

bright yellow colour developed within 20 min and after 1 h the dichloromethane was removed in vacuo. The residue was held under vacuum for 2 h to ensure that any residual *p*-tolylisocyanide was removed. The dry residue was taken up in dichloromethane, 5 ml, and ethanol, 20 ml, and lithium perchlorate, 0.03 g, were added. Concentration in vacuo lead to the formation of bright yellow crystals which were recovered by filtration, and then washed with ethanol, isopropanol and n-hexane, to give pure **8a**, 0.7 g, 63%, m.p. 159–160 °C. Anal. (as  $\frac{1}{3}$  dichloromethane solvate as confirmed by  $^1\text{H}$  NMR) Found: C, 65.32; H, 5.40; N, 2.37.  $\text{C}_{60}\text{H}_{51}\text{ClN}_2\text{O}_5\text{P}_2\text{Ru} \cdot \frac{1}{3}\text{CH}_2\text{Cl}_2$  calcd.: C, 65.46; H, 4.71; N, 2.53%. Crystals suitable for X-ray diffraction were grown from dichloromethane/ethanol.

$[\text{Os}(\text{C}(o\text{-tolyl})\text{OCH}_2)\text{Cl}(\text{CO})(\text{PPh}_3)_2]$  (**9**)

The preparation of this complex was described in the preparation of **7d**. The dichloromethane solution eluted from the column chromatography separation was diluted with ethanol, 20 ml, and bright yellow needles of **9**, 0.01 g, 10%, formed after concentration in vacuo. M.p. 173–175 °C. Anal. (as 1/1 dichloromethane solvate as confirmed by  $^1\text{H}$  NMR) Found: C, 56.08; H, 4.85.  $\text{C}_{46}\text{H}_{39}\text{ClO}_2\text{OsP}_2 \cdot \text{CH}_2\text{Cl}_2$  calcd.: C, 56.65; H, 4.16%.

*Crystal structure determinations*

For **5a** data were collected on a CAD-4 diffractometer at 25 °C and for **2d** and **8a** data were collected at –150 and –140 °C respectively on a Nicolet diffractometer. Crystallographic details are given in Table 1. For both **5a** and **8a** the space group  $P2_1/n$  was uniquely determined by systematic absences. For **2d** the structure was satisfactorily solved and refined in space group  $Pca2_1$ . In each case the data were corrected for Lorentz and polarization effects. Absorption corrections were applied by the empirical  $\psi$  scan method [49].

The structures were solved by conventional Patterson and difference Fourier techniques with SHELX, which determined the coordinates of all non-hydrogen atoms. The perchlorate anion in **8a** is markedly disordered and was modeled by two anions in different orientations (B and C in Table 12) in a 2/1 ratio. Full-matrix least squares refinement, with anisotropic thermal parameters for all non-hydrogen atoms except for the triphenylphosphine carbon atoms of **2d** and **5a**, converged to  $R = 0.039$ ,  $R_w = 0.039$  for **2d**,  $R = 0.049$ ,  $R_w = 0.048$  for **5a** and  $R = 0.067$ ,  $R_w = 0.076$  for **8a**. Final atomic positional parameters are listed in Tables 4, 9 and 12.

**Acknowledgements**

John Christiansen, Ward R. Robinson and William E.B. Shepard are thanked for their assistance in obtaining some of the crystallographic results. We would also like to acknowledge the New Zealand University Grants Committee for their grants towards instrumentation. One of us (D.S.B.) would also like to acknowledge their assistance in the form of a Postgraduate Scholarship. Finally, we would also like to thank Johnson Matthey for a generous loan of  $\text{OsO}_4$ .

**References**

- 1 L.J. Guggenberger, R.R. Schrock, *J. Am. Chem. Soc.*, 97 (1975) 6578.
- 2 A.F. Hill, W.R. Roper, J.M. Waters, A.H. Wright, *J. Am. Chem. Soc.*, 105 (1983) 5939.

- 3 A.T. Patton, C.E. Strouse, C.B. Knobler, J.A. Gladysz, *J. Am. Chem. Soc.*, 105 (1983) 5804.
- 4 M.D. Fryzuk, P.A. MacNeil, S.J. Rettig, *J. Am. Chem. Soc.*, 107 (1985) 6708.
- 5 R.R. Schrock, *J. Am. Chem. Soc.*, 97 (1975) 6576.
- 6 W.-K. Wong, W. Tam, J.A. Gladysz, *J. Am. Chem. Soc.*, 101 (1979) 5440.
- 7 W.E. Buhro, M.C. Etter, S. Georgiou, J.A. Gladysz, F.B. McCormick, *Organometallics*, 6 (1987) 1151.
- 8 W.E. Buhro, A.T. Patton, C.E. Strouse, J.A. Gladysz, *J. Am. Chem. Soc.*, 105 (1983) 1056.
- 9 M. Brookhart, W.B. Studabaker, *Chem. Rev.*, 87 (1987) 411.
- 10 D.L. Thorn, *Organometallics*, 1 (1982) 879.
- 11 J.C. Calabrese, D.C. Roe, D.L. Thorn, T.H. Tulip, *Organometallics*, 3 (1984) 1223.
- 12 H. Kletzin, H. Werner, O. Serhadli, M.L. Ziegler, *Angew. Chem., Int. Ed. Engl.*, 22 (1983) 46.
- 13 K. Roder, H. Werner, *Angew. Chem., Int. Ed. Engl.*, 26 (1987) 686.
- 14 D.L. Thorn, T.H. Tulip, *J. Am. Chem. Soc.*, 103 (1981) 5984.
- 15 D.L. Thorn, T.H. Tulip, *Organometallics*, 1 (1982) 1580.
- 16 R.C. Brady, R. Pettit, *J. Am. Chem. Soc.*, 102 (1980) 6181.
- 17 W.A. Herrmann, *Angew. Chem., Int. Ed. Engl.*, 21 (1982) 117.
- 18 D.S. Bohle, G.R. Clark, C.E.F. Rickard, W.R. Roper, W.E.B. Shepard, L.J. Wright, *J. Chem. Soc., Chem. Commun.*, (1987) 563.
- 19 W.R. Roper, L.J. Wright, *J. Organometal. Chem.*, 142 (1977) C1.
- 20 W.R. Roper, G.E. Taylor, J.M. Waters, L.J. Wright, *J. Organometal. Chem.*, 182 (1979) C46.
- 21 W.R. Roper, G.E. Taylor, J.M. Waters and L.J. Wright, *J. Organometal. Chem.*, 157 (1978) C27.
- 22 W.A. Herrmann, B. Reiter, H. Biersack, *J. Organometal. Chem.*, 97 (1975) 245.
- 23 J.P. Collman, L.S. Hegedus, *Principles and Applications of Organotransition Metal Chemistry*, University Science Books, Mill Valley, 1980.
- 24 G.R. Clark, T.J. Collins, K. Marsden, W.R. Roper, *J. Organometal. Chem.*, 259 (1983) 215.
- 25 M.A. Gallop, W.R. Roper, *Adv. Organometal. Chem.*, 25 (1986) 121.
- 26 J. Clemens, M.L.H. Green, F.G.A. Stone, *J. Chem. Soc., Dalton Trans.*, (1973) 1620.
- 27 G.E. Taylor, Ph.D. Thesis, University of Auckland, 1979.
- 28 D.S. Bohle, T.C. Jones, C.E.F. Rickard, W.R. Roper, *Organometallics*, 5 (1986) 1612.
- 29 G.R. Clark, K. Marsden, W.R. Roper, L.J. Wright, *J. Am. Chem. Soc.*, 102 (1980) 6570.
- 30 W.R. Roper, L.J. Wright, *J. Organometal. Chem.*, 234 (1982) C5.
- 31 W.R. Roper, J.M. Waters, L.J. Wright, F. van Meurs, *J. Organometal. Chem.*, 201 (1980) C27.
- 32 T.A. Albright, *Tetrahedron*, 38 (1982) 1339.
- 33 E.A. Carter, W.A. Goddard, *J. Am. Chem. Soc.*, 109 (1987) 579.
- 34 E.A. Carter, W.A. Goddard, *Organometallics*, submitted.
- 35 M.D. Curtis, K.-B. Shiu, W.M. Butler, *J. Am. Chem. Soc.*, 108 (1986) 1550.
- 36 C.A. Tolman, S.D. Ittel, A.D. English, J.P. Jesson, *J. Am. Chem. Soc.*, 100 (1978) 4080.
- 37 L. Pauling, *The Nature of the Chemical Bond*, Oxford University Press, London, 1960, p. 111.
- 38 S. Gambarotta, C. Floriani, A. Chiesi-Villa, C. Guastini, *Organometallics*, 5 (1986) 2425.
- 39 M.L.H. Green, M. Ishaq, R.N. Whiteley, *J. Chem. Soc. A*, (1967) 1508.
- 40 J. March, *Advanced Organic Chemistry*, McGraw-Hill, New York, 2nd edit., 1977.
- 41 L.E. Friedrich, P.Y.-S. Lam, *Tetrahedron Lett.*, 21 (1980) 1807.
- 42 E.O. Fischer, *Adv. Organometal. Chem.*, 14 (1976) 1.
- 43 A. Davison, J.P. Solar, *J. Organometal. Chem.*, 166 (1979) C13.
- 44 L.F. Friedrich, P.Y.-S. Lam, *J. Org. Chem.*, 46 (1981) 306.
- 45 W.R. Roper, *J. Organometal. Chem.*, 300 (1986) 167.
- 46 D.S. Bohle, W.R. Roper, *Organometallics*, 5 (1986) 1607.
- 47 D.S. Bohle, G.R. Clark, C.E.F. Rickard, M.J. Taylor, W.R. Roper, *J. Organometal. Chem.*, submitted.
- 48 Th.J. de Doer, W.L. Jolly, *Org. Synth.*, 4 (1963) 250.
- 49 A.C. North, D.C. Phillips and F.S. Mathews, *Acta. Cryst. A*, 24 (1968) 351.